Autoimmune Addison's Disease and DNA Methylation

Identification of Differentially Methylated Regions and Development of Methylation Specific PCR for Selected Genes

SHAHINUL ISLAM

This thesis is submitted in partial fulfilment of the requirements for the degree of Master in Medical Cell Biology

Department of Biomedicine
Faculty of Medicine and Dentistry
University of Bergen
Bergen, Norway
2012

Acknowledgement

The present work was carried out at the Department of Biomedicine, Faculty of Medicine and Dentistry, University of Bergen, Norway.

Before anything else, I would like to thank Professor Marit Bakke for being an excellent supervisor! You have always been encouraging and optimistic, and your knowledge and enthusiasm has been truly inspiring for me. By giving me chance to attend International conference, you taught me how the science is working globally and how international collaboration influence the quality of scientific work through knowledge sharing and communication. Even with a tightly packed schedule, you always found the time for helpful guidance throughout this period.

I would also like to thank my co-supervisor Trine Elholm Bjånesøy. You have been an invaluable oracle in the lab, and I always met a smiling face when I came to your office with all my questions and concerns. The opportunity to share the thought with you made me more curious to learn about science.

Great thanks to my research group, Bakke Research Lab, for creating a friendly and supportive atmosphere. Especially thanks to Torild Ellingsen for helping me with technical issue in the lab and to Dr. Erling A. Høivik for valuable discussion regarding PCR in DNA methylation analysis.

To my parents; thank you for putting me up and influencing me (genetically and environmentally), and to my consort for always supporting and believing in me although not fully understanding what my education and daily life aims at.

Finally, to all my fellow students – the last two years have been Excellent!

Shahinul Islam
June 2012

Table of contents

Abbreviations

AAD	Autoimmune Addison's Disease
ACTH	Adrenocorticotropic Hormone
AID	Autoimmune Disease
AIRE	Autoimmune Regulator
AMPK	5' AMP-Activated Protein Kinase
APECED	Autoimmune Polyendocrinopathy, Candidiasis and Ectodermaldystrophy Syndrome
APS	Autoimmune Polyendocrinopathy Syndromes
BH3	Only Pro-Apoptotic Bcl-2 Family Member
biPCR	Nested bisulphite PCR
Bim	Bcl-2 *Protein* Family Member
BWS	Beckwith-Wiedemann syndrome
BSP	Bisulphite Sequencing
CD	Cluster of Differentiation
CGI	CpG-island
CpG	Cytosine Followed by Guanine
CIITA	Class II, Major Histocompatibility Complex, Transactivator
CTL	Cytotoxic T Lymphocyte
CTLA4	Cytotoxic T-Lymphocyte Antigen 4
DHEA	Dehydroepiandrosterone
DM	Diabetes Mellitus
DMR	Differentially Methylated Region
Dnmts	DNA Methyl Transferases
FLCN	Folliculin
FNIP1	Folliculin Interacting Protein 1
FNIP2	Folliculin Interacting Protein 2
FNIPL	Folliculin Interacting Protein 1-like
FoxP3	Forkhead Box P3
GRIN2B	N-methyl-D-Aspartate Receptor Subunit 2B
HDAC	Histone Deacetylase

HLA	Muman Leuckocyte Antigen
HMT	Histone Methyltransferase
ICF	Intracellular Fluid
ITP	Idiopathic Thrombocytopenic Purpura
IPTG	Isopropyl-β-D-1-Thiogalactopyranoside
MADS-box	Conserved Sequence Motif Found in a Family of Transcription Factors
MAPO1	O(6)-methylguanine-Induced Apoptosis 1
MBDCap	Methylated DNA-Binding by Protein
MeDIP	Methylated DNA Immunoprecipitation
MeDIP-chip	Methylated DNA Immunoprecipitation Microarray
MeDIP-seq	MeDIP and High-throughput Sequencing
MEF2	Myocyte Enhancer Factor-2
MHC	Major Histocompatibility Complex
MIC A	MHC Class I Chain Related A
MS	Multiple Sclerosis
MSP	Methylation Specific PCR
mTOR	Mammalian Target of Rapamycin
NMDA	N-Methyl-D-Aspartate
NK	Natural Killer Cells
PEG3	Paternally-Exoressed Gene 3
PTPN22	Protein Tyrosine Phosphatase, Non-receptor Type 22 (lymphoid)
qPCR	Quantitative PCR
RAC1	Ras-related C3 Botulinum Toxin Substrate 1
RAR	Heumatoid Arthritis
RCC2	Regulator of Chromosome Condensation 2
SAM	S-adenosylmethionine
SLC30A10	Solute Carrier Family 30 Member 10
SLE	Systemic Lupus Erythematosus
Th17	Helper T-cells 17
TNFSF7	Tumor Necrosis Factor Ligand Superfamily, Member 7
T_{REG}	Regulatory T-cells
TSS	Transcription Start Site
WGA	Whole Genome Amplification

Abstract

Autoimmune Addison's Disease (AAD) is a classical organ-specific autoimmune disease (AID) that is characterized by autoreactivity towards the adrenal cortex, leading to insufficient production of steroid hormones and death if left untreated. The genetic factors that contribute to AAD development are not well characterized, and it is commonly accepted that epigenetic factors are involved in the onset of AAD, as they are for other autoimmune diseases. This master project was part of a larger project that aims to identify genomic regions that are differentially methylated in AAD patients compared to control individuals through the use of methylated DNA immune precipitation in combination with gene array (MeDIP-chip). DNA methylation is a major epigenetic component that is essential for gene expression in embryonic development, normal physiology and disease. Differential methylation status is associated with various pathological conditions, such as cancers and autoimmune diseases. Therefore, precise mapping of the methylome has become a crucial issue to understand gene expression.

The MeDIP-chip approach generated a list of genomic regions that are differentially methylated in patients and controls. Some of these regions were analyzed *in silico* for the position in the corresponding gene and to gain insights of the epigenetic properties of the specific region. The major part of this thesis work involved the development of methylation specific PCR (MSP). This method was developed for the purpose to verify the MeDIP-chip data and to allow screening of large cohorts of both AAD patients and other autoimmune diseases. MSP protocols, in which different primer sets specifically hybridized with either unmethylated or methylated DNA was developed for five genomic regions. Moreover, one region was analyzed by bisulphite sequencing. Bisulphite seqeuncing is widely used to generate single CpG site methylation maps, but it became evident that it is not suitable for methylation analyses of a large quantity of samples. DNA from five patients and five control individuals were analyzed with MSP across a region in the FLCN gene that was found to be hypermethylated in AAD patients in the MeDIP-chip. Interestingly, this differentially methylated region was localized to a CpG-island shore, suggesting regulatory effects of the methylation status. The MSP analysis partly verified a different level of methylation in patients and controls, but the results strongly suggest that quantitative MSP needs to be developed for the genomic regions of interest to be able to distinguish between differences

hypo- and hypermethylation. Taken together, the work presented in this master thesis contributed to the identification of genomic regions that are differentially methylated in patients with AAD and healthy controls, and developed methodology that will be an important tool for further evaluation of aberrant methylated regions in patients with autoimmune diseases after some further refinement.

Introduction

1. Epigenetics and DNA Methylation

The term "epigenetics" was first used in 1957 by Conrad H Waddington (1905-1975) and stated: "*Epigenetics is the branch of biology that studies the causal interactions between genes and their products, which bring the phenotype into being*". The modern view of epigenetics has become narrower, which is now commonly used to refer to heritable traits that affect gene expression but that are not caused by the underlying DNA sequence. The following definition was posted by Russo in 1996:*"The study of mitotically and/or meiotically heritable changes in gene function that cannot be explained by changes in DNA sequence" (Russo et al.1996).*

Epigenetics comprises a variety of modification processes, which can cause long term or short term on gene expression programs, and is involved in the regulation of all biological processes from conception to death (Handel, Ebers et al. 2010). The major components in epigenetics are DNA methylation and histone modification. These modifications can interplay with each other and with other mechanisms like non-coding RNAs and regulatory proteins (Delcuve, Rastegar et al. 2009). Histone modifications can be characterized in two different ways either by affecting the contact between different histones in adjacent nucleosome or the interaction of histones and DNA. Both approaches are affecting chromatin structure. The nucleosome is the fundamental unit of chromatin and is composed of a octamer of histones wrapped with 147 bp double-stranded DNA (Kouzarides 2007). Histone with DNA wrapped tightly regulates genome sequence from abnormal gene expression or modification. Structural orchestrations of chromatin are either euchromatin or heterochromatin. Euchromatin is characterized by high level of histone acetylation mediated by histone acetyl transferases (HATs) and the genes can be actively transcribed. Transcriptional repression is mediated by altering of acetylation by the enzyme histone deacetylases (HDACs). The silencing of euchromatin converts the chromatin to heterochromatin, which then is enriched by H3 trimethylation recruited by histone methyltransferase (HMTs). DNA methylation in the promoter region of a gene in euchromatin can however block transcription factors association with DNA and thereby regulates the initiate of transcription.

1.1 DNA Methylation

DNA methylation is a post-replicative DNA modification where a methyl group is added to the 5`position of cytosine (C) residues in the DNA backbone. The reaction is carried out by a group of enzymes known as DNA methyltransferases (Dnmts) that uses S-adenosylmethionine (SAM) as methyl-donor (figure_1). In eukaryotes, DNA-methylation occurs almost exclusively at CpG dinucleotides [*i.e.* where C is followed by a guanine (G) in the DNA sequence], although it has been demonstrated that methylation can also occur on C followed by A and T, especially in embryonic stem cells (Ramsahoye, Biniszkiewicz et al. 2000). DNA methylation is common in plants, and in addition to a high frequency of CpG methylation, methylation also occurs in CHG and CHH (H is A, C or T) in plants (Zhang, Kimatu et al. 2010). In invertebrates, the type and frequency of DNA methylation varies, depending on if they have Dnmts or not (Glasted et al. 2011)

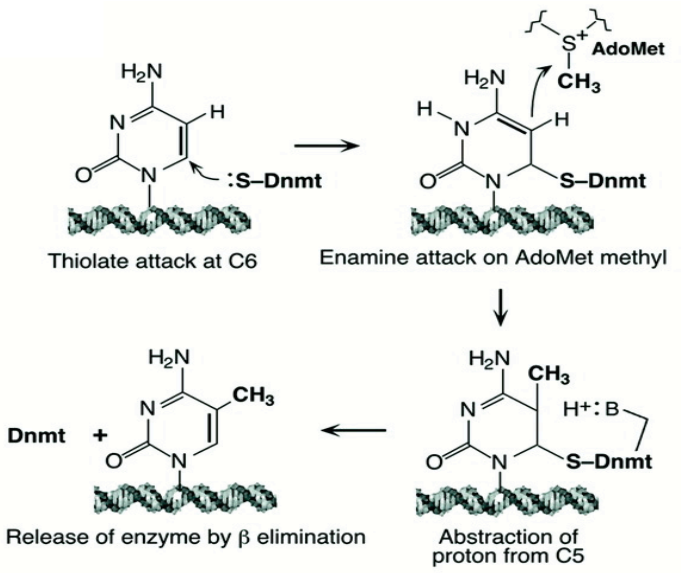

(Bestor 2000)

Figure_1: Enzymatic mechanism of DNA methylation.

DNA methylation pattern is inherited because the Dnmt1 is present at the replication fork. There are other DNA methyl transferases that carry out de novo methylation including Dnmt3a and Dnmt3b. The fact that Dnmt3a and Dnmt3b are also essential for life is proved by mouse knockdown studies. Mice that lack of Dnmt3a die within a few weeks after birth and different DNA methylation pattern in somatic tissue where non-CpG methylation following CpA and CpT is diminished due to low level of Dnmt3a and Dnmt3b *(Li, Bestor et al. 1992; Okano, Bell et al. 1999).*

1.2 Biological processes controlled by DNA methylation

Initial studies demonstrated important roles for DNA methylation in genomic imprinting, X chromosome inactivation and heterochromatin maintenance (Bestor 2000). In more recent years it has also become evident that waves of demtehylation/remethylation are essential for normal embryonic development. These processes are described briefly below:

Genomic imprinting: Genomic imprinting is a process that ensures that a gene is expressed in a parent-of–origin specific manner *(Robertson 2005)*. About 100 imprinted genes have been characterized in mammals and most of them are identified in clusters *(Weaver, Susiarjo et al. 2009)*. For instance, human 11p15.5 domain contains a large cluster of imprinted genes, and abnormal methylation of some genes within this cluster results in Beckwith-Wiedemann syndrome (BWS) (Verona, Mann et al. 2003). DNA methylation is the best characterized epigenetic mark involved in the allele-specific expression of imprinted gene, and this mechanism is particularly important during paternal sperm development and postnatal oocyte maturation *(Bartolomei and Ferguson-Smith 2011)*. Many developmental processes depend on that only either the maternal or paternal gene is expressed such as for PEG3 gene. This gene is imprinted and thereby not expressed from the maternal allele but expressed from the paternal allele. The precise function of PEG3 is not clear but might be involved in p53/c-myc-mediated apoptosis pathway (Kohda, Asai et al. 2001; Dowdy, Gostout et al. 2005; Feng, Marquez et al. 2008).

X-chromosome inactivation: In mammals, males contain one X-chromosome and one Y-chromosome, whereas female contain X chromosomes. The X-chromosome is gene-rich, and many genes are not involved in other processes than sex determination and reproduction. Expression of the genes from both X chromosome in the female would cause imbalance of gene expression between the sexes and have great impact on metabolic mechanism (Gartler and Goldman 2001). Already in 1931, H. J. Muller et al. posted that mammals and some other species have evolved a system to bring about the equivalence in expression of X-linked genes in females and males. DNA methylation plays a key role in X-chromosome inactivation by imposing hypermethylation in promoter regions. Studies in somatic cell hybrids show that promoter methylation is one of two critical factors in maintaining silencing on the inactive X chromosome. For an instance, promoter hypomethylation in DNMT3B (DNA methyltransferase gene) in the inactive X-chromosome results Immunodeficiency,

centromeric instability and facial anomalies (ICF) syndrome (Ehrlich, Jackson et al. 2006). It is interesting to note, that overall, the inactive X-chromosome is not hypermethylated compare to the active one, rather the hypermethylation is targeted to specific regions (Gartler and Goldman 2001).

Heterochromatin maintenance: Heterochromatin is defined as highly compacted nuclear materials as opposite to the less-condensed euchromatin, and it is believed to be hypermethylated. DNA methylation also plays important role in heterochromatin maintenance. Both constitutive and facultative heterochromatin is involved in transcriptional silencing of genes by DNA methylation along with other functions. Cytosine within heterochromatin are highly methylated and, the hypermethylated status act synergistically with chromatin modifications to achieve a repressed chromatin stage (figure_2).

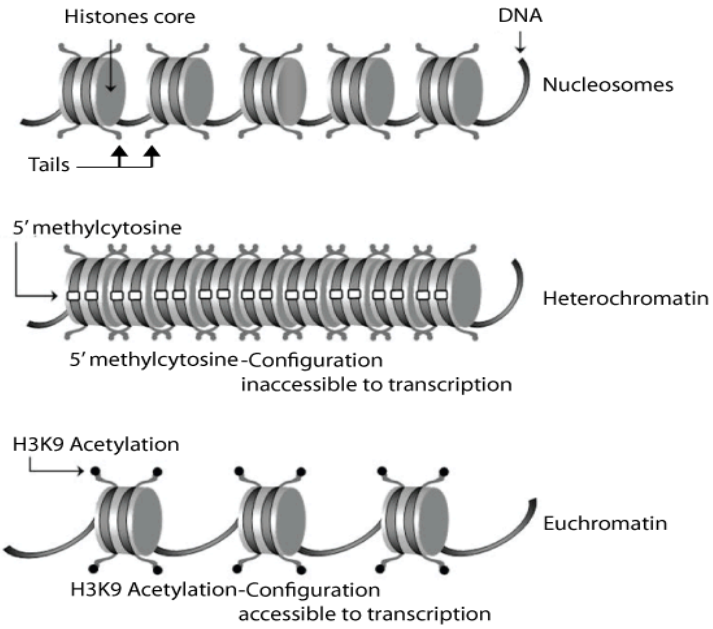

Figure_2: The role of DNA methylation in heterochromatin maintenance. Heterochromatin is inaccessible to transcription due to increased level of cytosine methylation mediated by histone methyl transferases (HMTs).

Whole genome studies have revealed interesting roles for DNA methylation in heterochromatin orchestration, and demonstrated that heterochromatin is less methylated than euchromatin in the highly repetitive juxtacentromeric sequence of the human genome *(Suzuki, Oda et al. 2011)*. This might indicate that DNA methylation is linked to chromatin organization where less methylation is needed for DNA kept “inaccessible” for transcription in heterochromatin and contrapositive for euchromatin.

DNA methylation in embryonic development: Diploid zygote formation of gametes during fertilization is the primary step of human development, and gametes and later on the zygote must go through a reconfiguration configuring all kind of modification. Two phases of global demethylation occurs during mammalian development by epigenetic reprogramming (figure_3). The first step takes place during germ cell development, which is associated with loss of DNA methylation including imprinted genes. The second step takes place after fertilization throughout preimplantation period of development, and is also associated with loss of DNA methylation excluding imprinted genes. Moreover, paternal and maternal DNA shows different pattern of losing DNA methylation just after zygote formation.

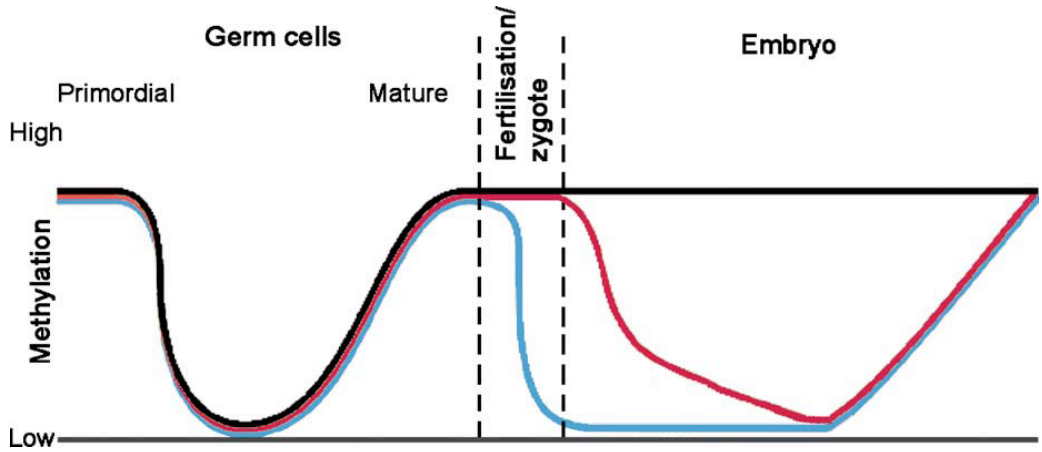

Figure_3: DNA methylation restoration program during embryonic development showing stable and inherited pattern of DNA methylation. The diagram depicts the methylation level in methylated (black line) imprinted and non-imprinted genes (red; maternal, blue; paternal) during germ cell and embryonic development.

(Dean, Santos et al. 2003)

1.3. DNA methylation and regulation of gene transcription

DNA methylation takes place as major epigenetic modification in respect to ubiquitous and tissue specific gene expression. Different transcription factor can bind to hypomethylated CpG sites in promoters and initiate transcription. Hypermethylated CpG rich promoters are unable to interact with the necessary factors to initiate transcription, and transcription is repressed. As described above, there is tight communication of DNA methylation and histone modifications, leading to either an open or close chromatin state (Kouzarides 2007). Genomic regions of 500-1000 base pairs that contain elevated levels of C and G, and little CpG depletion are referred to as CpG-islands (CGI). The total number of CGIs in human genome is around 25500 (Illingworth, Gruenewald-Schneider et al. 2010). It is also evident that almost half of the CGIs are located in promoters of annotated genes overlapping the

transcription start site *(Deaton and Bird 2011)*. CGIs are often found in promoters of housekeeping genes and are generally kept hypomethylated, regardless of the transcriptional activity of the gene. Around 5% of CGI-promoters exhibit a tissue differentially methylation pattern, but the majority of genes that are expressed in a tissue-restricted pattern are controlled by promoter containing few CpG sites (also denoted weak CGIs) (Shen, Kondo et al. 2007; Irizarry, Ladd-Acosta et al. 2009; Illingworth, Gruenewald-Schneider et al. 2010). The roles of CGIs in tissue specific gene expression are emerging and it is now known that not all CGIs with a regulatory function are located to promoter area (figure_4). Genome-wide analysis reveals their genomic distribution and indicated both intragenic and intergenic location. CGIs with no known function are named orphan CGIs, but they might as well be important in gene regulation. Another surprising finding through large-scale analysis is that many orphan CGIs contain novel promoters (Maunakea, Nagarajan et al. 2010; Deaton and Bird 2011).

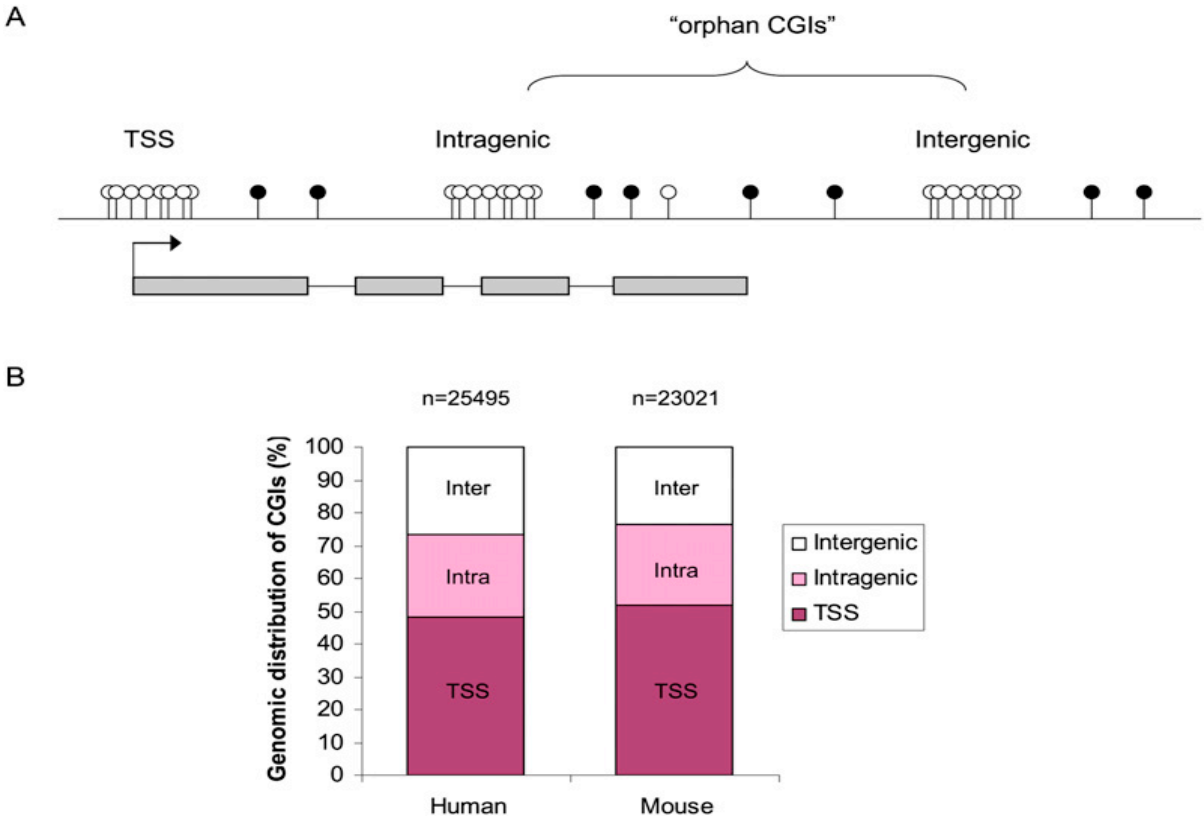

Figure_4: Gene transcription regulation by CGIs.

A. Location of CGIs throughout the human and mouse genome; TSSs, intragenic or intergenic. Unmethylated CpG are indicated by empty lollipops and methylated CpG by filled lollipops. B. The genomic distribution of CGIs in the human and mouse genome as determined in ((Illingworth, Gruenewald-Schneider et al. 2010), figure from *(Deaton and Bird 2011)*.

1.4. DNA Methylation and disease

Environmental factors, though epigenetic mechanisms, play important roles in the connection between genetic susceptibility and disease development. Life style, food habit and environment can promote either hypermethylated or hypomethylated DNA by providing or removing methyl groups, which might be the principle reason to develop disease condition due to abnormal DNA methylation (table_I).

Table_I: Environmental factors affecting the epigenome

Environmental factor	Evidence for epigenetics
Methyl donor (folate, vitamin B12, choline, betadine)	Administration to mice causes changes in coat colour mediated by altered DNA methylation in region near Agouti gene (*Wolff, G.L. et al. 1998 & Cooney, C.A. et al. 2002)*.
Sex hormones	Endocrine toxin causes inheritable defects in DNA methylation-mediated spermatogenesis in rats (*Anway, M.D. et al. 2005).* Perinatal exposure of human infants to diethylstilbesterol causes epigenetic increase in malignancy (*Li, S. et al. 2003).*
Smoking	Paternal parent-of-origin transgenerational effects on obesity in sons is highly suggestive of epigenetic changes *(Pembrey, M.E. et al. 2006).*
Nutrition	Parent-of-origin transgenerational effect on mortality in sex-matched offspring is highly suggestive of epigenetic changes *(Pembrey, M.E. et al. 2006).*
Vitamin D	Vitamin D receptor binding complex can cause epigenetic changes *(Issa, L.L. et al. 1998).*
Stress	Stressful upbringing causes epigenetic changes in glucocorticoid receptor promoter region in rats (*Weaver, I.C.G. et al. 2004).* Childhood abuse associated with epigenetic changes in glucocorticoid receptor promoter region in human suicide victims *(McGowan, P.O. et al. 2009).*

This table shows environmental factors that could result in epigenetic changes.

Moreover, unlike genetic changes, which are permanent, autoimmune disease (AID) related epigenetic modifications are reversible and this can be potential reason to develop epigenetic

therapies to treat complex and polygenic diseases. These changes can also be inherited over generation (Ballestar, Esteller et al. 2006). Loss of normal DNA methylation pattern in somatic cells results in loss of growth control and hypomethylation and is a hallmark of cancer *(Robertson 2005)*. Alternatively, DNA methylation can repress genes, which are responsible for disease. 'Epimutation', which is abnormal silencing of gene, is the most potent example of genetic susceptibility to DNA methylation (Martin, Ward et al. 2005).

2. Autoimmune Addison's disease

Autoimmunity develops because of defects in the immune system in which the normal process of self-antigen recognition is disturbed. The immune systems start a defence towards own cell components because it recognizes self-proteins as foreign molecules. Central tolerance is the ability of newly formed T and B cells to recognize but not respond to self-antigens, and this ensure negative selection. Negative selection is the process, by which high affinity T-cells deletion occurs. High affinity T-cells are capable of recognizing self-antigens and mount a strong immune response against them. Breakdown of central tolerance is the principle explanation of autoimmunity. Autoimmune disorders is third highest burden for clinical manifestation in the world *(Nossal 2001)* and 3-7% of the population in Europe and United states are suffering from an autoimmune diseases *(Jacobson, Gange et al. 1997; Marrack, Kappler et al. 2001)*. Multiple sclerosis (MS), systemic lupus erythematosus (SLE), diabetes mellitus (DM), autoimmune haemolytic anaemia, Rheumatoid arthritis (RA), autoimmune Addison's disease (AAD), autoimmune polyendocrinopathy syndromes (APS) are the most common autoimmune diseases.

Addison's disease (AD) refers to primary adrenocortical insufficiency and is a life-threatening disorder first noticed by Thomas Addison in 1885 *(T Addison 1855)*. In most cases, AD is caused by autoimmunity and is then referred to as Autoimmune Addison's disease (AAD). AAD is an organ specific autoimmune disease where the target organ is adrenal gland *(Betterle 2002; Myhre, Undlien et al. 2002; Arlt and Allolio 2003)*. Adrenal cortex destruction occurs by an unknown mechanism and as the disease progresses fibrous tissue replaces the cortex. This leads to hampered steroid hormone production and finally complete lack of cortical hormone production. The healthy adrenal gland consists of an outer cortex and an inner medulla. The cortical portion produces steroid hormones that are essential for life, and therefore, if left untreated, AAD is lethal. The cortex consists of three different zones; the outer zona glomerulosa that produces mineralo corticoids, the middle zona

fasciculata that produces glucocorticoids and inner zona reticularis that produces adrenal androgens (figure_5). Aldosterone is the most common and important mineralocorticoid and is essential for the regulation of water and salt balance and maintenance of blood pressure. Cortisol is the principle glucocorticoid and has profound effects on almost every organ in human body including cardiovascular, metabolic, immunologic and homeostatic function *(Sapolsky, Romero et al. 2000)*.

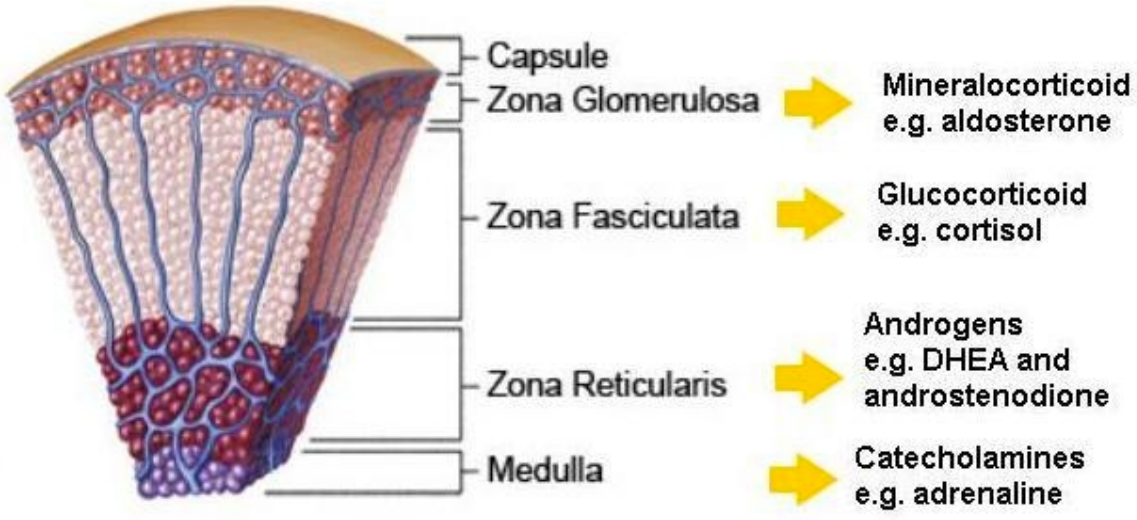

Figure_5: Microscopic section of Adrenal gland.

The prevalence of AAD and Addison's disease (AD) in general worldwide is not well documented, and most likely many patients are undiagnosed (*Ian Ross and Naomi Levitt 2011*). Thereafter, the estimation for autoimmune Addison's disease is 100-140 per million and incidence rates of 5-6 per million *(Martina M Erichsen et al. 2009; Delves and Roitt 2000; Janeway 2001; Medzhitov 2007)*, while about 90-140 peoples per million are suffering in western countries *(Ten, New et al. 2001; Lovas and Husebye 2005)*. The western part of Norway has a somewhat higher incidence and the rate is increasing with time *(Lovas and Husebye 2005)*. In general, autoimmune diseases are caused by multiple genes dysfunction, and most of the autoimmune diseases are coexisted with at least one additional immune disorder *(Neufeld, Maclaren et al. 1981)*. For instance, about 50-60% of Addison's patient have at least one additional clinical or preclinical autoimmune disorder like diabetes type I, APS I or APS II *(Betterle, Lazzarotto et al. 2004)* and cardiovascular disease as well *(Ian Ross and Naomi Levitt 2011)*. Interestingly, APS type II is defined as AAD in conjunction with autoimmune thyroid disease and /or type I diabetes. APS type I is known as autoimmune

polyendocrinopathy, candidiasis and ectodermal dystrophy syndrome; APECED. Thus, Addison's patient comorbidity suggests genetic susceptibility of the disease.

During the 160 years that have passed since the first identification of AD, there have been excellent diagnostic advances and a remarkable understanding of the mechanism at the molecular level. Hormone replacement therapy has been available from 60 years ago (*Ian Ross and Naomi Levitt 2011*). However, AAD is still a potential lethal condition if overlooked, many die due to adrenal failure. The mortality rate is excessively higher in young people due to acute adrenal insufficiency, sudden death and most likely because of infection (Erichsen, Lovas et al. 2009). The clinical manifestations of AAD patients are non-specific and diagnosis can be difficult. Tiredness with muscular weakness is the main reason why patients seek medical attention. The two most characteristic symptoms are hyper pigmentation and salt craving. The age of diagnosis is usually in forth decade of life *(Arlt and Allolio 2003).* An overview of the clinical features of AD patients is given in table_II.

Table_II: Clinical features of Addison's disease

Symptoms	Signs	Biochemical abnormalities
Fatigue	Postural hypotension	High (supine) plasma renin and/or increased nighttime ACTH levels
Muscular weakness	Weight loss	Low ACTH stimulated cortisol responses
Abdominal pain	Generalized pigmentation, darkened skin creases, pigmented buccal mucosa and nail beds	At the time of crisis: normo-or hyponatremia, hyperkalemia, hypoglycemia Eosinophilia
Vomiting	Associated vitiligo and/or goiter	
Diarrhoea		Lymphocytosis
Salt craving		
Behavior changes		
Headache, Sweating		
Depression,		
Muscle and pain		

(Ten, New et al. 2001)

2.1 Molecular and genetic characteristics of AAD

It is established that AAD patients have over expression of T-cells and antibody producing B-cells. The importance of T-cells differentiation in AAD pathogenesis is illustrated by the fact that patients present with increased percentage of T-cells along with decreased percentage of regulatory T-cells (T_{REG}) *(Rabinowe, Jackson et al. 1984; Coles, Thompson et al. 2005)*. A major breakthrough in AAD research was the identification of antibodies against P450 21-hydroxylase in the majority of AAD patients *(Soderbergh, Gustafsson et al. 2006)*. Adrenal antigen specific T cell have been recognised both in adrenal gland and in peripheral blood *(Nerup, Andersen et al. 1969; Nerup and Bendixen 1969)*. T-cell response against adrenal specific protein fraction and the microsomal fraction as well has demonstrated *(Nerup and Bendixen 1969; Nerup, Andersen et al. 1970; Ludwig, Eibl et al. 1976; Freeman and Weetman 1992)*. It is not understood why immunoreactivity against P450 21-hydroxylase is associated with AAD, besides that this enzyme is essential for steroid hormone production in the adrenal cortex (Krohn, Uibo et al. 1992; Winqvist, Gustafsson et al. 1993).

The genetic origin of AAD is not well understood, but has been linked to some genes essential for the immune system. The present knowledge indicates that AAD is, as most autoimmune diseases, a polygenic disorder. Single nucleotide polymorphism (SNP's) studies from different populations revealed the relation between certain class of HLA haplotype and AAD *(Maclaren and Riley 1986; Myhre, Undlien et al. 2002; Gombos, Hermann et al. 2007)*. The risk is increased in the presence of the HLA-DRB1*404 allele where one or two single amino acid alterations increased antigen peptide presentation by MHC II *(Gregersen, Silver et al. 1987)*. MHC class I chain related A (MIC A) has also been linked to the development of AAD, as it is involved in up regulation of natural killer cells (NK) and cytotoxic T lymphocytes (CTLs) function *(Stephens 2001; Spies 2002)*. CTLA4, CIITA and PTPN22 are also genes related to increased risk for AD. All these genes to AD encode proteins that are involved in regulation of antigen specific T-cells and they are also associated with other autoimmune diseases *(Brand, Gough et al. 2005)*.

3. DNA methylation and autoimmunity

Environmental factors, through epigenetic mechanisms, are believed to contribute to the increased prevalence of autoimmune diseases that are observed in industrial societies (Veldhoen and Duarte 2010). Only about one-third of the risk of developing an autoimmune disease might be caused by genetic factors, and the influence of the environment is evident by the discordant penetrance of autoimmune diseases in monozygotic twins (Ballestar 2010). The stochastic selection of TCRs is also important as well as non-genetic causes (Gronski, Boulter et al. 2004). The best-studied autoimmune diseases with regard to DNA methylation are the Silver-Russel and Beckwith-Weidemann syndromes (Verona, Mann et al. 2003). In both these syndromes, hypomethylation is observed. Several studies have focused on the importance of the DNMTs and how they might be involved in autoimmunity (Meda, Folci et al. 2011). DNMT-activity is impaired in B and T-cells in SLE patients (Brooks, Le Dantec et al. 2010).

In the immune system, several pathways that play major roles in lymphocyte proliferation and differentiation are regulated by DNA methylation *(Adam E. Handel et al. 2009)*. For instance, CD40L, which is Cluster of Differentiation 40 (glycoprotein), is overexpressed in women with SLE and manifest a demethylation of the corresponding gene on the inactivated X-chromosome (Meda, Folci et al. 2011). Hypomethylation of the TNFSF7 promoter causes over activation of CD4+ T-cells followed by B-cells activation and autoantibody production with subsequent organ damage in SLE patient (Zhou, Qiu et al. 2011). Although DNA methylation has been demonstrated to be involved in other autoimmune disease, and play important roles in T-cell biology and differentiation, it has not been investigated with regard to AAD before.

Aims of the Study

The work presented in this master thesis was the part of a project where the major aim is to identify genomic regions that are differentially methylated in patients with AAD. MeDIP-chip analyses identified genomic regions that were either hypo- or hypermethylated compared to controls. These regions where situated most frequently in CpG-islands, but were also found in CpG-island shores, gene promoters, introns, exons and in intergenic regions.

The specific aims were:

1) Contribute to the MeDIP-chip by preparing DNA and MeDiP of control samples.

2) Characterize *in silico* a selected number of genetic regions identified in the MeDIP-chip with regard to genetic location (as specified above), and examine the existing literature to identify potential links to autoimmunity or the immune system.

3) Establish a protocol of methylation specific PCR (MSP) for a selected number of genomic regions.

4) Establish bisulphite sequencing (BSP) for a selected number of genomic regions.

Materials

1. Oligonucleotides applied in PCR as primers

Table_III: PCR primers used for MSP

Gene & Primer	Sense primer (5'--3')	Antisense primer (5'--3')	Size, bp
FLCN, M	GTCGTGTTTTGGTAATAGTTTC	ATTACAAACGTAAACCACTACG	181
FLCN, U	GGTTGTGTTTTGGTAATAGTTTT	AATTACAAACATAAACCACTACA	181
HDAC4, M	GTTTATGAGATTTTGTCGGC	ACGATAACTCCAACGAACTC	112
HDAC4, U	TGGTTTATGAGATTTTGTTGGT	AAACAATAACTCCAACAAACTC	112
SLC30A10, M	CGAAGATTTTGAAGGGGAAC	CGTAAAATATAACCTCATCCGC	170
SLC30A10, U	TAGTGAAGATTTTGAAGGGGAAT	CATAAAATATAACCTCATCCACCAC	170
GRIN2B, M	ATAAATACGGCGTGGTTAGC	CCGAATACACGCCTACCTA	170
GRIN2B, U	GATAAATATGGTGTGGTTAGT	ACCAAATACACACCTACCTA	170
RCC2, M	AGTGTTTTGGTGCGGAATC	CGACCTAAACAACACAACGAA	121
RCC2, U	AGTGTTTTGGTGTGGAATT	CAACCTAAACAACACAACAAA	121

M represents methylated-specific primers and U, unmethylated-specific primers.

Table_IV: Primers used in nested PCR

Gene & Primer	Sense primer (5'--3')	Antisense primer (5'--3')	Size, bp
FoxP3, O	AGTGGGATGTACCCAGCTAC	ATAGAGCTTCAGATTCTCTTTCTTT	652
FoxP3, N	GGCCCCATTGGAGGAGAT	TCAGATGACTCGTAAAGGG	360

O represents- primers for outer region and N, nested primers.

Table_V: Primers used in sequencing

Identification Name	Direction	Target Region	Sequence
201	R	SP6 (pGEM)	GGAAACAGCTATGACCATGATTA

2. Bacterial strain used and medium

Table_VI: E.Coli strain

Bacterial Strain	Provider	Genotype
DH5α	Stratagene, USA	F- endA1 glnV44 thi-1 recA1 relA1 gyrA96 deoR nupG Φ80d*lacZ*ΔM15 Δ(*lacZYA-argF*)U169, hsdR17(rK- mK+),λ–

Table_VII: Bacteria growth medium

Medium for Ampicillin Selection	Contents
LB- medium	Bacto- Tryptone (10%), Difco BD, USA Bacto-Yeast Extract (5%), Difco BD, USA NaCl (0.17 M), Merck, Germany Ampicillin (100 μg/ml), Sigma, USA
LB-plates	LB-medium Agar (15%) provided by *BIO-RAD* Laboratories Inc., USA

3. Chemicals, molecular biology reagents and kits

Table_VIII: Modifying enzymes

Name	Supplier
GoTaq® Flexi DNA Polymerase	Promega, USA
T4 DNA ligase	Promega, USA

Table_IX: Plasmid

Name	Insert	Provider
pGEM	Amplified bisulphite treated fragment	Promega, USA

Table_X: Molecular weight standards

Name	Supplier
100 bp DNA Ladder	New England Biolabs, USA
1 kb DNA Ladder	New England Biolabs, USA

Table_XI: Chemicals and supplementary

Chemical and Reagents	Supplier
Molecular Biology Agarose	*BIO-RAD* Laboratories Inc., USA
Bromophenol Blue (0.042% bromophenol blue, 0.042% xylene cyanol FF, 2.5% Ficol 400)	Merck, Germany
Ampicillin and Ethidium Bromide	Sigma, USA
Bacto-Yeast extract	Difco BD, USA
X-Gal	Promega, USA
Isopropyl β-D-1-thiogalactopyranoside (IPTG)	Promega, USA
Ethanol	Arcus, Norway
Iso-propanol	Arcus, Norway
TAE buffer (40 mM Tris, 0.1% Acetic acid, 1 mM EDTA (pH 8.0))	Prepared in the Lab

Table_XII: Molecular biology kits

Name	Supplier	Catalogue No.
Dynal®CD4 Positive Isolation Kit	Invitrogen, USA	113.31D
MagMeDIP Kits (48x^{TM})	Diagenode, Belgium	mc-Magme-048
DNeasy blood and tissue kit (250)	Qiagen, USA	69506
IPure DNA Isolation Kit (250)	Diagenode, Belgium	AL-100-0100
GenomePlex® Complete Whole Genome Amplification (WGA) Kit	Sigma, USA	070M6184
E.Z.N.A Plasmid Mini Kit (250 preps)	Omega Bio-Tek, USA	D 6942-02
QIAquick® Gel Extraction Kit	Qiagen, USA	28706
QIAquick® PCR Purification Kit (250)	Qiagen, USA	28106
MinElute® PCR Purification kit (250)	Qiagen, USA	28006
EZ DNA Methylation-Gold kit^{TM}	Zymo Research, USA	D5006

4. Technical instruments

Table_XIII: Equipments

Instrument	Use	Manufacturer
BioRad Gene Pulser II	Electroporation	*BIO-RAD* Laboratories Inc., USA
MJ Research PTC-200	PCR	*BIO-RAD* Laboratories Inc., USA
Innova 4430	Bacterial Shaker	New Brunswick Scientific, USA
NanoDrop Spectrophotometer	DNA Concentration Measurement	Thermo Scientific, USA
Bioruptor	Sonication	Diagenode, Belgium
BIO-RAD iCycler	Quantitative PCR	*BIO-RAD* Laboratories Inc., USA
Transluminator	UV Transmitter	Fujifilm, Japan
Incubator (Termaks)	Incubator	Thermo LAB, India

5. Computer software

Table_XIV: Software utilities

Software Specification		Developer
Clustal X 2.0.10	Alignment of Sequence	Conway Institute UCD Dublin, Ireland
BioEdit 7.0.9.0	Visualization of chromatograms	Ibis Therapeutic, USA
Methyl Primer Express®	Primer Design	Applied Biosystems, USA
Reverse Complement Software	Make DNA Complimentary	http://www.geneinfinity.org/sms/sms_reversecomplement.html
Adobe Illustrator CS4	Sequence Editing Software	M Microsoft Incorporation, USA

Methods

1. Patients

The patient DNA used in this study was obtained from a Norwegian bio-bank and registry on patients with Addison's disease, directed by Dr. Husebye, Dept of Medicine, Haukeland University Hospital, Bergen, Norway. The control DNA was obtained from healthy blood donors via the blood bank of Haukeland Hospital. 10 patients with confirmed AAD was analyzed in the MeDiP-chip (Human DNA Methylation 2.1M Deluxe Promoter Array, NimbleGen Roche, Inc.). Informed consent had been obtained by Dr. Husebye for genetic studies, and the Regional Committee for Ethics in Medical Research (REK149/96) had approved the investigation.

2. Methylation specific polymerase chain reaction

MSP is probably the most sensitive non-quantitative method due to its capability to detect 0.1% methylation or less at any block of CpG sites (Rand, Qu et al. 2002; Kristensen, Mikeska et al. 2008). The method is outlined in figure_6(A and B) is essential that the primers that recognize methylated DNA. The unique characteristic of methylated primer pair facilitate to distinguish methylated DNA sequence in a background of unmethylated DNA, and the unmethylated primer pair only amplify the unmethylated DNA.

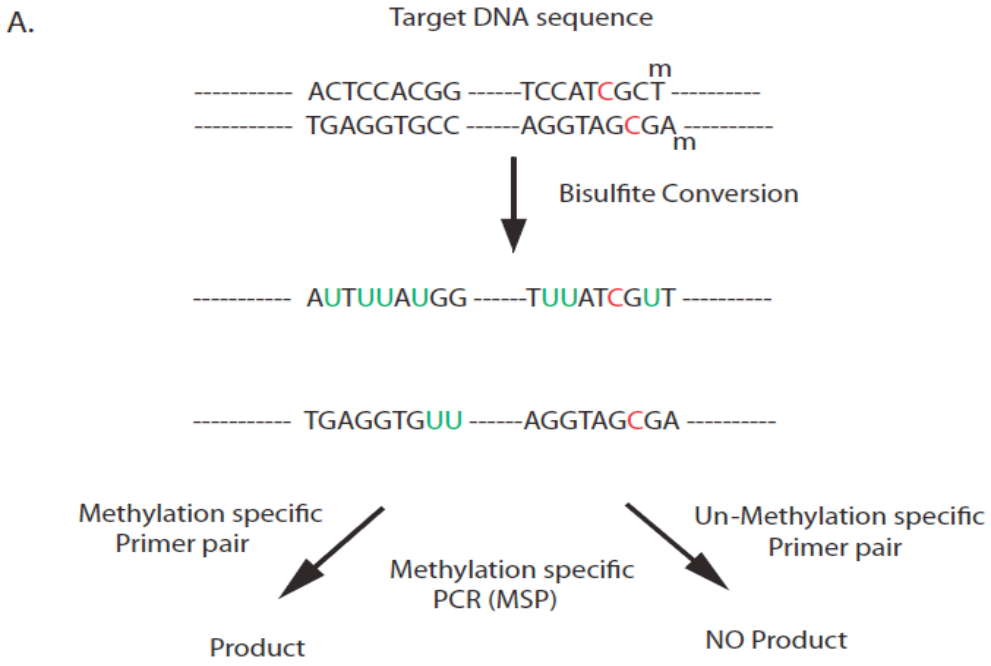

Figure_6A: Principle of methylation specific PCR (MSP) for methylated DNA.

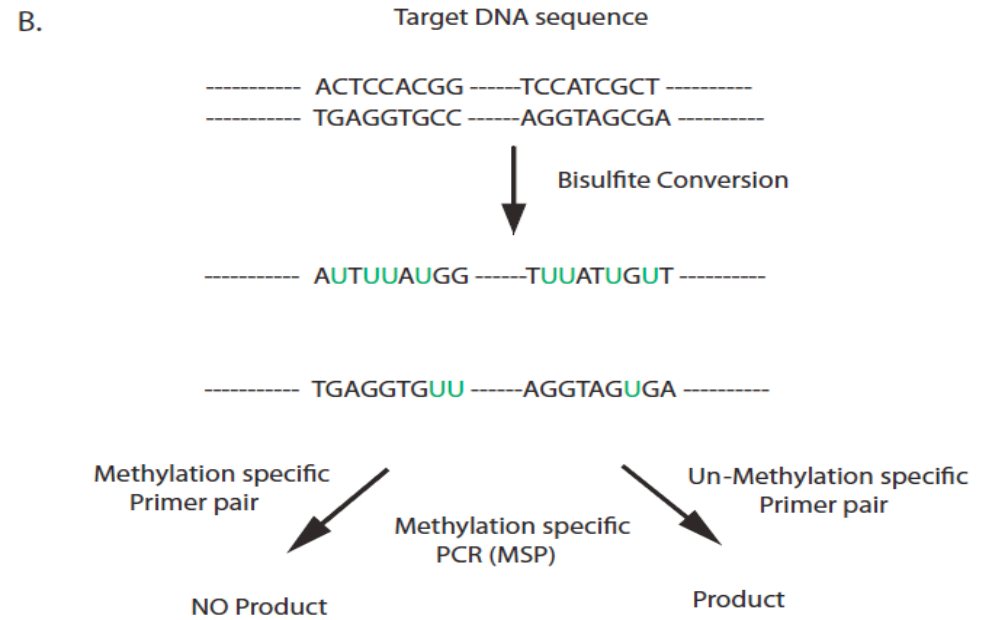

Figure_6B: Principle of methylation specific PCR (MSP) for methylated DNA.

3. Positive isolation of CD4+ T-Cells from blood

Dynal® CD4 positive isolation kit was used to isolate CD4+ T-cells from blood from patients and controls. This kit is based on a primary monoclonal antibody specific for the CD4 membrane antigen. Whole blood was washed with buffer 1 (PBS, with 0.1% BSA and 2mM EDTA but without Ca^{2+} and Mg^{2+}, pH 7.4) to remove interfering soluble factors present in the plasma fraction. Dynabeads CD4 are uniform magnetic polystyrene bead coated with CD4+ T-cells specific primary antibody that will capture the CD4+ T-cells. Before use, the Dynabeads were prepared by washing with buffer 1. The ration between Dynabeads and washed whole blood was $5x10^6$ Dynabeads to 1 ml of blood. The isolated CD4+ T-cells were then washed three times with buffer 1 and resuspended in 100 μl Buffer 2 (RPMI 1640/1% FCS)/ml blood.

DETACHaBEAD was used to detach the bead from the CD4+ T-cells. DETACHaBEAD CD4 is a polyclonal anti-Fab antibody specific for the CD4 primary antibody and is supplied with the kit. Detached beads were removed from the sample with additional wash steps with buffer 2 and a magnet. Isolated CD4+ T-cells were then transferred in Buffer 2 (500 μl) and cell number was determined by counting in a Bürker chamber.

3.1. Purification of DNA from isolated CD4+ T-cells

DNA from isolated CD4+ T-cells was purified by using the Qiagen DNeasy Blood & Tissue Kit. Cells (maximum 5×10^6) were first incubated with adequate amount of proteinase K and RNase A (100 mg/ml) at room temperature for 2 min. Protienase K is a serine protease that digests the proteins including nucleases, and therefore protects nucleic acid from degradation. RNase A catalyses the degradation of RNA and thus removes RNA from the sample. The cells where then lysed in buffer AL and incubated in this lysis buffer for 30 min at 58°C. 70% ethanol was added, and the samples were applied to silica-based membrane columns that bind DNA to remove contaminants and enzyme inhibitors. The columns were washed with buffer AW1 and buffer AW2. The DNA was then eluted in elution buffer (200 μl). The concentration of the purified DNA was determined by a NanoDrop fluorospectrophotometer. The purified DNA was stored at 4°C.

4. Immunoprecipitation of methylated DNA (MeDIP)

The Diagnode MagMeDIP kit was used to immunoprecipitate (IP) methylated DNA. The method is a genome-wide, high-resolution approach to detect and isolate methylated DNA. Enriched methylated DNA can be interrogated using DNA microarray. Purified DNA (10 μg) was dissolved in elution buffer (200 μl) and sonicated to produce fragments of 300-500 bp. The sonication intervals were 15 seconds 'ON' and 15 seconds 'OFF' for 15 minutes. To verify that the DNA was shared, the sonicated DNA (0.1 μg in 1x DNA loading dye; 0.007% bromophenol blue, 0.007% xylene cyanol FF, 0.42% Ficol 400) was analyzed by agarose gel electrophoresis (1%) in 1x TAE buffer. The sonicated DNA was prepared for IP with a buffer supplied with the kit, and control DNA and the anti-methylcytosine antibody used to precipitate methylated DNA was diluted to 1:2 with water according to manufacturer's instructions.

Before IP, the DNA was denatured at 95°C, to allow for binding of the antibodies, and quickly chilled on ice. 10% of this sample was separated for input and kept at 4°C before further downstream preparation. The washed and prepared Magbeads capable to bind the antibody and the antibody mixture was then added and the reaction was incubated overnight on a rotating wheel at 4°C. The next morning, the IP reactions were washed three times with ice-cold MagWash buffer-1 (100 μl; detergent, salt anion chelator mix incubated) in a cold room. Each wash consisted of resuspension by inverting the tubes, incubation for 4 minutes at 4°C on a rotating wheel (40 rpm), collection of the beads by centrifugation and incubation in the magnetic rack for 1 minute before the buffer was discarded. The detergent mix in the MagWash buffer-1 helps to dissolve nuclear membranes around the DNA and the salt mixture denatured any remaining DNase. The captured beads were kept attached to the tube wall. The beads were washed again with ice-cold MagWash buffer-2 (100 μl; detergent, salt anion chelator mix) by following the procedure stated above, and the beads were kept on ice.

4.1. Purification of MeDIP DNA

The MeDIP isolated DNA was purified and eluted from the antibody-beads by the Diagnode IPure kit. This kit is commonly used to purify DNA for downstream application like hybridization to microarray. Elution buffer (1:1 mix of buffers A and B provided by the kit) were added to the bead pellet (50 μl) and the input sample (92.5 μl elution buffer to 7.5 μl input sample) and incubated for 15 minutes at RT on a rotating wheel (40 rpm). The samples

were centrifuged briefly in a microfuge and placed into the DiaMag2 magnetic rack for 1 minute. The methylated DNA containing supernatant was collected into new tubes and the elution was repeated once. Iso-propanol (100 μl) and a carrier able to bind DNA and the magnetic beads was added to each IP reaction and input sample together with magnetic beads (15 μl) and incubated for 1 hour at RT on a rotating wheel (40 rpm). The bead-bound DNA was then washed with wash buffer 1 and wash buffer 2 according with a short incubation (1 minute) at room temperature on a rotating wheel (40 rpm). The DNA was eluted in buffer C (supplied with kit) in a total of 50 μl (two elusions, each 25 μl). The concentration of eluted DNA was measured by UV fluorospectrophotometry (NanoDrop). Magnetic beads were kept in liquid suspension at 4°C at all times, as drying will result in reduced performance.

5. Whole genome amplification

As hybridization to NimbleGen Human DNA Methylation 2.1M Deluxe Promoter Array required 6 μg of DNA, the MeDIP-DNA was amplified by the GenomePlex® Complete Whole Genome kit. According to the manufacturer, this kit amplifies the entire genomic DNA with minimum amplification bias. The starting amount of DNA is critical, and according to the kit, 10 ng is optimal. When using a complex starting material, such as human genomic DNA, the gene bias in the resulting GenomePlex product is significantly altered if the quantity of input DNA is reduced. The first step in the GenomePlex® Complete Whole Genome kit is to convert the immunoprecipitated fragments into PCR-amplifiable units flanked by universal adaptor sequences. These modified fragments (that together makes up the OmniPlex library) are then subjected to a limited number of PCR cycles to produce enough material hybridization to the array. The procedure was followed according to the manufacturer's recommendation. In short, 10 ng of DNA was used for each amplification. Fragmentation buffer provided by the kit (1 μl) was added to the DNA (10 ng) followed by denaturation at 95°C for 4 minutes.

The OmniPlex library DNA was then generated by using the library preparation enzyme (1μl) and library solution buffer (2 μl) in the stepped isothermal reactions as follows below:

Table_XV: The OmniPlex library generation isothermal cycles

Temperature (°C)	Incubation time (min)
16°C	20 minutes
24°C	20 minutes
37°C	20 minutes
75°C	5 minutes
4°C	Hold

Amplification accompanied by following the cycle below:

Table_XVI: The profile of thermocycling in amplification

Steps	Temperature	Incubation time	Cycles
Initial Denaturation	95°C	3 minutes	× 1
Denaturation Anneal/Extension	94°C 65°C	15 seconds 5 minutes	× 14

The final WGA DNA was stored at - 20°C and is as stable as any genomic DNA sample.

5.1. Purification of WGA DNA

The amplified DNA contains primers, nucleotides, polymerases and salts that must be removed before DNA array hybridization. The Qiagen MinElute PCR Purification kit performed this. Five volumes of binding buffer PB was mixed with one volume of PCR reaction and transferred onto MinElute column following centrifugation (13000xg) for one minute. Column bound DNA was then washed with wash buffer (750 μl) and centrifuged for one minute. One additional one-minute centrifugation was carried out to remove residual ethanol from wash buffer. Double-distilled water (10 μl) was applied directly to the column matrix and left for one minute before centrifugation to elute the DNA.

6. Quantitative real time PCR

To verify the immunoprecipitation and amplification of methylated DNA, quantitative PCR (qPCR) on known methylated and unmethylated region was performed. qPCR was used because this method can determine the concentration of a certain transcript in the sample. qPCR is based on detection of a fluorescent signal produced proportionally during the amplification of a PCR product.

qPCR of isolated DNA was carried out by using the iCycler software where isolated DNA (10 µl) was applied with primer pair (reverse and forward) by following the qPCR cycle below:

Table_XVII: The delineation of temperature cycle during qPCR reaction

Steps	Temperature	Incubation time	Cycles
Amplification	95°C	7 minutes	×1
	95°C	15 seconds	×40
	60°C	60 seconds	
	95°C	1 minute	×1
Melting curve	65°C and increment of 0.5°C per cycle	1 minute	×60

7. Microarray analysis

Microarray technology has become one of the most powerful tools for biological research and also widely used in methylation analysis because of its high throughput manner. DNA methylation microarrays are specialized microarray technology used to measure provided DNA methylation by hybridizing with probes attached to a solid surface. Each probe contains a specific DNA sequence corresponding this project; the Human DNA Methylation 2.1 M Deluxe Promoter Array from NimbleGen Roche was used. This array covers CpG-islands and promoters. This array requires around 6 µg of input DNA, with an optimal concentration of 250-500 µg/µl. The WGA DNA was sent to NimbleGen (Reykjavik, Iceland) for hybridization. The raw microarray data was processed and analyzed by Dr. Bettina Andreassen at the department of Biostatistics, University of Oslo. An overview of the MeDIP procedure followed by WGA and microarray is shown in appendix I.

8. Bisulphite conversion

DNA methylation detection is essential for the study of epigenetic changes in the genome. Several methods have been developed to analysis DNA methylation, and methods applying bisulphite conversion are the most commonly used techniques. This is accomplished by temperature denaturation to replace chemical denaturation with sodium hydroxide, which causes unmethylated cytosine to be converted into uracil while methylated cytosine remain unchanged. The amount of DNA per treatment can range from 500 pg to 2 µg and an optimal amount is 200-500 ng regarding the instruction given EZ DNA Methylation-Gold Kit. The purified genomic DNA (500 ng) of CD4+ T-cells was treated with sodium bisulphite salt (130

μl; dissolved in M-dissolving buffer and M-dilution buffer, provided by the kit). The conversion was performed in a thermal cycler following the conditions below:

Table_XVIII: The denaturation temperature cycles for bisulphite treatment

Step	Temperature (°C)	Incubation time
Denaturation	98°C 64°C 4°C	10 minutes 2.5 hours Storage up to 20 hours

The purification of converted DNA was achieved by using Zymo-spin IC silica membrane column together with M-binding buffer (600 μl). M-binding buffer bind the DNA to the column and the column was washed once with washing buffer containing absolute ethanol (100 μl) before desulphonation in M-desulphonation buffer (200 μl) provided by the kit. The desulphonation step prevents precipitation of bulky DNA. The DNA was washed again to stop the desulphonation reaction and eluted by spinning briefly after a short incubation with elution buffer provided by the kit (10 μl). It is important to minimize template degradation and loss of DNA during treatment and cleanup, and this was assured by thoroughly following the procedures given by the manufacturer's recommendation. The DNA was then ready for immediate analysis of nested PCR followed by cloning and sequencing or MSP.

9. Methylation specific PCR (MSP)

The amplification mix was prepared (1.25 unit of DNA Polymerase enzyme, 1 mM $MgCl_2$, 1x buffer (yellow dye), 10 mM dNTP, 20 mM forward primer and 20 mM reverse primer) and added with 100 ng DNA sample in a 25 μl PCR reaction. The following PCR settings were as shown in table_XIX:

Table_XIX: The profiles of isothermal cycles in Methylation specific PCR

Step	Temperature (°C)	Incubation time	Number of cycles
Initiation	95°C	5 minutes	
Denaturation Annealing Elongation	95°C 55-60°C 72°C	30 seconds 30 seconds 30 seconds	35 cycles
Final extension End	72°C 4°C	4 minutes Forever	

The fragments amplified by MSP were analyzed by agarose gel electrophoresis as described below.

10. Nested bisulphite PCR (biPCR)

Nested bisulphite PCR (biPCR) is often used when bisulphite treated single stranded DNA is the template because this template is fragile. According to the principle of nested PCR, the use of two primer sets will highly increase the specificity of the amplification. For the second round, amplified DNA from the first round was used as DNA template with the same settings. The application mix contained 100 ng of DNA in a 25 µl PCR reaction (1.25 unit of DNA Polymerase enzyme, 1 mM $MgCl_2$, 1x buffer (yellow dye), 10 mM dNTP, 10 mM forward primer and 10 mM reverse primer). The settings were as shown in table_XX.

Table_XX: The profiles of isothermal cycles in bisulphite PCR

Step	Temperature (°C)	Incubation time	Number of cycles
Initiation Denaturation Annealing Elongation	96°C 96°C 57.4°C 72°C	2 minutes 30 seconds 45 seconds 1 minute 30 seconds 2 minutes	5 cycles
Denaturation Annealing Elongation Final extension End	95°C 57.4°C 72°C 72°C 4°C	30 seconds 1 minute 30 seconds 1 minute 30 seconds 10 minutes Forever	30 cycles

11. Agarose gel electrophoresis

Agarose gel electrophoresis is a method used to separate DNA according to size. The method is frequently used after PCR to visualize and isolate the amplified fragments. DNA separation occurs by applying an electricity field to the gel. The negatively charged DNA molecules migrate towards the positive cathode. The fragments were visualized on 2.5% agarose gels prepared in 1xTAE buffer. To visualize DNA in a transluminator, ethidium bromide (10 µl) was added. Ethidium bromide becomes interchalated into the DNA strand, and works as fluorescent tag under UV-light. A 100 bp ladder was used as the molecular weight marker.

12. Gel extracted DNA purification and cloning

Gel extraction of the fragments amplified in the nested PCR was carried out to purify the fragments for downstream applications. Excised gel pieces (150-200 mg) was dissolved in QG buffer supplied with the QIAquick Gel Extraction Kit by 10 minutes at 57°C incubation and vortexing every second minute. QG buffer is a solubilization and binding buffer with pH indicator, which can confirm the pH and efficient for absorption of the DNA to the QIAquick membranes remaining yellow. The DNA is washed with the ethanol containing wash buffer PE and eluted by applying elution buffer (40 µl; 10mM Tris-Cl, pH 8.5). Elution efficiency is dependent on pH and the maximum elution efficiency is achieved between pH 7.0 to 8.0. The DNA fragments (6.5 µl) of interest were ligated into the pGEM vector in the presence of DNA ligase enzyme (2 µl) following incubation for half an hour in room temperature. After desalting by using cellulose membrane for 15 minutes at room temperature. Desalting was performed because salt can reduce the transformation efficiency.

12.1. Transformation of E.coli

Transformation into DH5α strain of *E.Coli* was performed by both heat-shock at 42°C and electroporation. Because of the hydrophobic bilayer core, DNA never passively diffuses across the cell membrane. The heat shock opens the pores of the bacterial cell wall and the plasmids can enter the cell. Placing the cells on ice after the heat shock closes the pores. The commercially available One®TOP10 chemically competent *E.coli* strain was used for heat-shock transformation. The bacteria and the pGEM vector containing the amplified fragment of interest was kept on ice before and after the heat shock. Desalted ligation reaction (20 µl) was transferred into One Shot® cells (50 µl) by mixing gently by tapping the tube. The mixture was incubated in ice for 5 min before incubation at 42°C for 30 sec, and then placed immediately on ice for 2 minutes. The sample was resuspended in pre-warmed S.O.C. medium (250 µl) and incubated at 37°C for 1 hour with shaking at 225 rpm.

Electroporation makes nm-scale water-filled holes in the bacterial cell wall by applying electric charge. The lipid molecules of membrane shift position, opening up a pore as a conductive pathway and allow the plasmid to enter the cell. After removing the charge, the pore close automatically. The electro competent strain of *E.Coli* (DH5α) was thawed on ice. Desalted ligation mix (20 µl) was mixed with bacteria (40 µl) by tapping the tube, and the reaction was transferred to a cuvette. Electroporation was carried out at 200 Ohms, 25 mF, 1.8

kV. The bacteria was resuspended in LB medium (1 ml) immediately and transferred to a 15 ml Falcon tube and incubated for 1 hour at 37°C in a shaking incubator at 225 rpm.

12.2. Blue-White screening

Blue-white screening is a method to identify bacterial clones that contain plasmids with successful ligation of the fragment of interest into the vector. After ligation and transformation the transformed bacteria are grown in the presence of X-gal. If the ligation is successful, the colony will be white because the reading frame of the LacZ gene is disrupted. Blue colonies are due to the presence of IPTG (Isopropyl-β-D-1-thiogalactopyranoside) in the growing substrate. The transformed bacterial cultures (100 µl or 200 µl) were plated onto LB plates containing ampicillin (100µg/ml), X-gal (80 µg/ml) and IPTG (80 µg/ml). For the pUC19 control, the transformation mix was diluted 1:10 into LB Medium (e.g. 100 µl of the transformation mix with 900 µl of LB Medium) before plating. The plates were incubated at 37°C for 17 hours.

12.3. Plasmid extraction

Successfully transformed single bacterial colonies were picked from selection plates and inoculated to in 5 ml LB medium containing ampicillin (100µg/ml) in 15 ml Falcon tubes for 14-20 hours at 37°C with vigorous shaking at 225rpm. Plasmids were isolated from inoculated cultures by using the E.Z.N.A® Plasmid Mini Kit. The bacteria were pelleted by centrifugation at 10000xg for one minute at room temperature and resuspended in solution I containing RNase A provided with the kit (250 µl). Solution-I contains glucose, Tris, and EDTA. Glucose is added to increase the osmotic pressure outside the cells. Tris is a buffering agent used to maintain a constant pH (8.0). EDTA protects the DNA from DNase; EDTA binds divalent cations that are necessary for DNase activity whereas RNase A is used to make RNA free solution. Complete resuspension (no visible cell clumps) of cell pellet is vital for obtaining good yields. Solution-II provided by the kit (250 µl) was then added and the samples were mixed gently by inverting and rotating tube to obtain a clear lysate. Vigorous mixing should be avoided because it can cause chromosomal shearing and potential contamination of genomic DNA and lower plasmid purity. Solution-II contains NaOH and SDS (a detergent). The alkaline mixture ruptures the cells, and the detergent breaks apart the lipid membrane and solubilizes cellular proteins. NaOH also denatures the DNA into single strands.

Next solution-III (350 µl), also provided by the kit, was added and the sample mixed by inverting several times until white precipitation was formed. It is vital that the solution is mixed thoroughly and immediately after the addition of solution III to avoid uneven precipitation. Solution-III contains a mixture of acetic acid and potassium acetate. The acetic acid neutralizes the pH, allowing the DNA strands to renature. The potassium acetate precipitates SDS from the solution, along with cellular debris. The *E. coli* chromosomal DNA is also trapped in the precipitate but the plasmid DNA remains in solution. The fractionation step following centrifugation for 10 minutes at 13000xg is carried out to separate the plasmid DNA from the cellular debris and chromosomal DNA in the pellet. The supernatant is added in an equilibrated HiBind DNA Mini Column. The plasmid DNA was then washed using DNA wash buffer (700 µl) and eluted by adding of MQ water (40 µl) after 1 min incubation. The plasmid concentration was determined with a NanoDrop fluorospectrophotometer.

13. DNA sequencing

The purified plasmids were sequenced using the BigDye kit to verify that the inserts were correct. The reaction mix contained DNA template (200 ng), reverse primer 201 (4 pmol), Big Dye (1 µl), sequencing buffer (µl) and H_2O to a total volume of 10 ml pursuing the sequencing set-up listed in Table_XXI. The plasmids were sequenced at the sequencing facility, SeqLab, at the University of Bergen. The sequencing data was analyzed by the ClustalX and BioEdit software to profile the DNA methylation in the target segment.

Table_XXI: Sequencing set-up for BSP sequencing

Step	Temperature (°C)	Incubation time	Number of cycles
Initiation	95°C	3 minutes	
Denaturation	96°C	14 seconds	
Annealing	58°C/48°C*	14 seconds	
Elongation	56°C	3 minutes	35 cycles
End	4°C	Forever	

Results

The major aim of this thesis was to develop methyl specific PCR (MSP) for specific genomic regions that were identified as differently methylated in patients with AAD compared to control individuals. The regions were identified by applying the MeDIP methodology in combination with gene array (Human DNA Methylation 2.1M deluxe promoter arrays from NimbleGen Roche, Inc). Preparation of genomic DNA from CD4+ T-cells and the MeDIP experiments were mainly performed by PhD-candidate Trine Bjånesøy, but I contributed to the procedure by preparing the samples from some control individuals. The different preparation and verification methods performed are described on page under "Methods", but the results from the intermediate steps from the DNA isolation and MeDIP are not shown here. Dr. Bettina Kulle Andreassen at University of Oslo performed the statistical analysis of the array data. The list of the differentially methylated regions that were identified is shown in appendix II. It is important to note that this list is based on the number of probes on the array that hybridize to a specific genomic region, meaning that the larger the genomic region that is differentially methylated between patients and controls, the better score this region will obtain. Moreover, all genomic regions listed in appendix II were found to be differently methylated in all patients and all controls. The MeDIP-chip data is based on array data from 10 AAD patients and 12 control blood donors.

However, before the data was processed by Dr. Andreassen, I analyzed a specific region in the promoter of the FoxP3 gene based on the data generated by NimbleGen. Both patients and control had DNA methylation in promoter sequence, but patient showed substantial more methylation in all patients compared to all controls. This region was analyzed by BSP as described below.

BSP analysis of the *FoxP3*

The gene encoding FoxP3 (*FoxP3*) was analyzed by nested PCR followed by bisulphate sequencing. FoxP3 is a transcription factor coding for Forkhead box protein P3 with key regulating function in the development of regulatory T-cells (Wang, de Zoeten et al. 2009). The gene contains 12 exones, and is located on the negative strand of the X-chromosome, according to UCSC genome browser (http://genome.ucsc.edu/). For all genes, NCBI/hg18, March-2006 assembly was used to localize the gene positions. It has been demonstrated that the DNA methylation status of the proximal promoter of *FoxP3* is associated with its expression (Li, Zhao et al. 2011). The region that was identified as hypermethylated in patients compared to controls is localized within the proximal promoter region around the transcription start site, as indicated in figure_7A. The identified region contains 14 CpG sites, but do not form a CGI according to the definition of Gardiner-Garden and Frommer (Gardiner-Garden and Frommer 1987). The setting were; length > 200 bp, GC content > 50%, the ratio of observed CpG/ expected CpG > 0.60. The outer BSP primers were designed as outlined in figure_7B. The nested primers amplified a region covering ten CpG sites (figure_7C). No significant difference in DNA methylation between two AAD patients and two controls individuals was found (figure_7D-H).

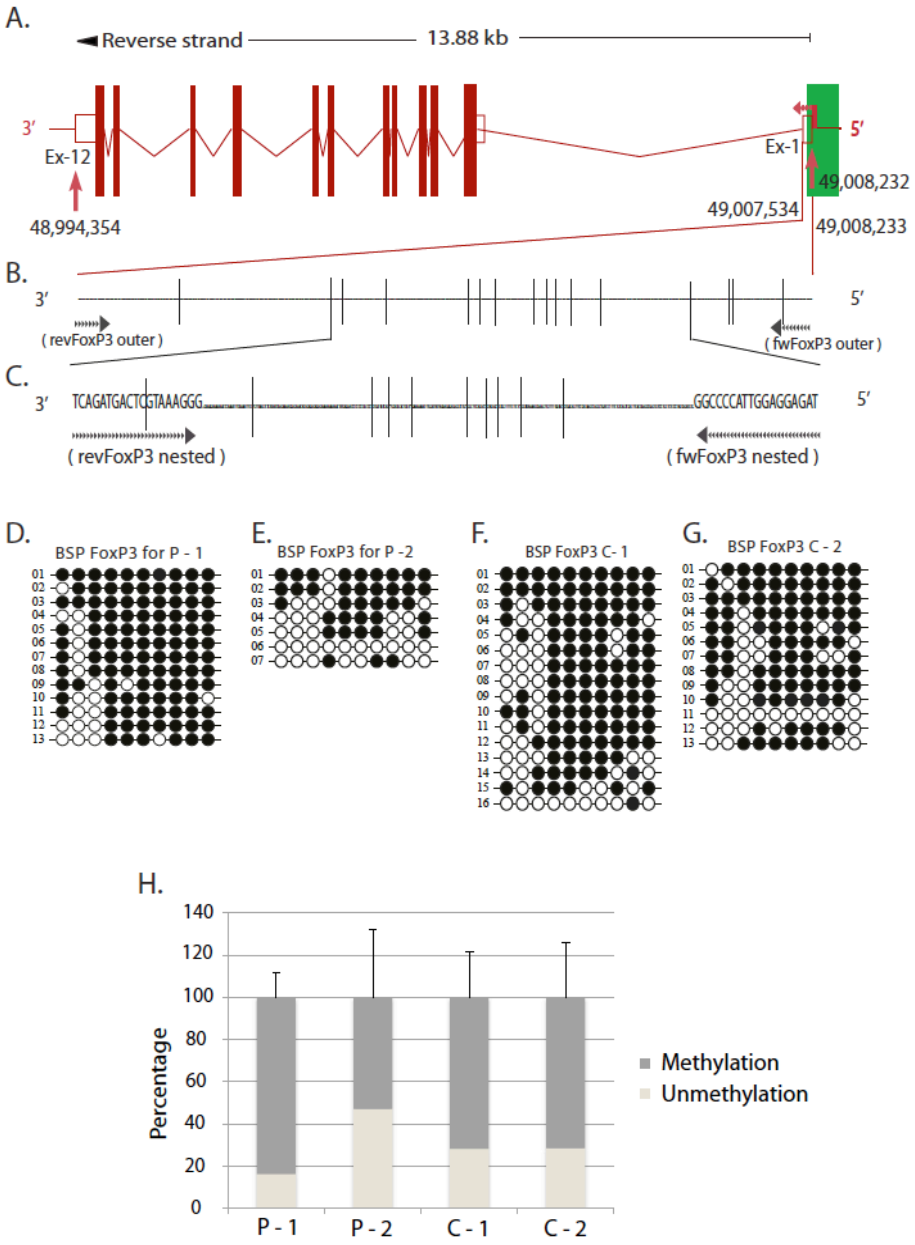

Figure_7: BSP analysis of *FoxP3*.

A: Schematic presentation of the FoxP3 gene with exons 1-12 indicated by coloured red bars. Associated promoter region have indicate by green bar. The gene is 13.88 kb long; spanning from position 49,008,232 to 48,994,354 on the X-chromosome. The transcriptional start site is marked by a broken arrow and the region found to be hypermethylated according to preliminary result from the MeDIP-chip is indicated by bordering with red lines from 49,008,233 bp to 49,007,534 bp. B: The region identified is highlighted and vertical lines indicate the CpG sites. Primers for first round PCR are indicated in B and the target region for nested primers bordered with black lines. C: The BSP-amplified sequence region is highlighted and the sequence and the name of primers are indicated; indicated primers binding sites (upper case) with covered CpG sites. D-G: Electrphoretic mobility analysis chart showing the result of the bisulphite sequencing analysis on DNA from two AAD patients and two control individuals. Each vertical line with circles represents one analysed clones, and each circle one CpG site (10 CpG sites). Black circles illustrate methylated CpG sites and white circles unmethylated CpG sites. H: The results in D-G are presented as percentage methylated with unmethylated as well. The bars represent the average of clones as mean +/– SD (n for P-1; 13, P-2; 7, C-1; 16, C-2; 13).

The reason for developing MSP for selected genes was that we wanted an efficient tool to verify the regions identified through the MeDIP-chip approach, and to be able to screen more patients, also from other cohorts. In short, the procedure was as follows:

1) Genomic regions from the array data was selected based on the known association to autoimmune diseases or because the nature of the differentially methylated region.
2) The selected genomic regions were analyzed *in silico* by the software UCSC genome browser (http://genome.ucsc.edu/) to determine if the region contained promoters, enhancers, CpG sites or CpG-islands.
3) By use of the Methyl Primer Express® software, primers were designed that would recognized either methylated or unmethylated DNA after bisulfite conversion. Primers that recognized unmetylated DNA are hereafter called 'unmethylated primers' and primers that recognized methylated DNA called 'methylated primers'.
4) PCR experiments were performed on completely methylated or unmethylated human DNA to verify their specificities.
5) The primer set developed for the gene encoding folliculin was tested on AAD patients and control individuals.

Primer design for Methylation Specific PCR (MSP)

The purpose of MSP is to determine the difference in methylation status focusing on a sequence of a specific genomic region in individuals in the case and control group. The applied primers must discriminate between methylated and unmethylated cytosine after bisulfite conversion so that the methylated primer pairs hybridize only to the methylated DNA, and unmethylated primer sets only to unmethylated DNA. Depending on the CpG content of the region of interest, primer design can be challenging. The Methyl Primer Express® software was used to design the MSP primers. In this software CGIs are identified according to the definition of Gardiner-Garden and Frommer (Gardiner-Garden and Frommer 1987); length > 200 bp, GC content > 50%, the ratio of observed CpG/ expected CpG > 0.60. The selected sequence that is used as input is modified *in silico* to mimic bisulfite modified DNA. It is important to take into account that the two strands will not be complimentary after bisulfite conversion. Methylated primers must cover a minimum of two CpG sites, and to get a more robust binding to the template, one CpG site should be located at the most 3'-end of

the primer. Unmethylated primers must cover the same CpG sites as the corresponding methylated primers. See table_III page 16 for primer sequences.

Preparation of unmethylated control DNA

The methylated control human DNA was purchased from New England Biolabs, USA. To prepare the unmethylated control DNA for MSP, genomic DNA was isolated from blood of a healthy donor. The DNA was subjected to fragmentation and amplified. Methylation is lost during whole genome amplification (WGA). Five reactions were run in parallel, and the quality of the WGA DNA was controlled by gel electrophoresis before purification. As shown in figure_8, all samples consisted of a smear in the range of 200-800 bp, with the mean size ~ 400 bp, which was requirement for downstream application. Importantly, this is the same range as control DNA (control in the most right lane), which was provided with kit.

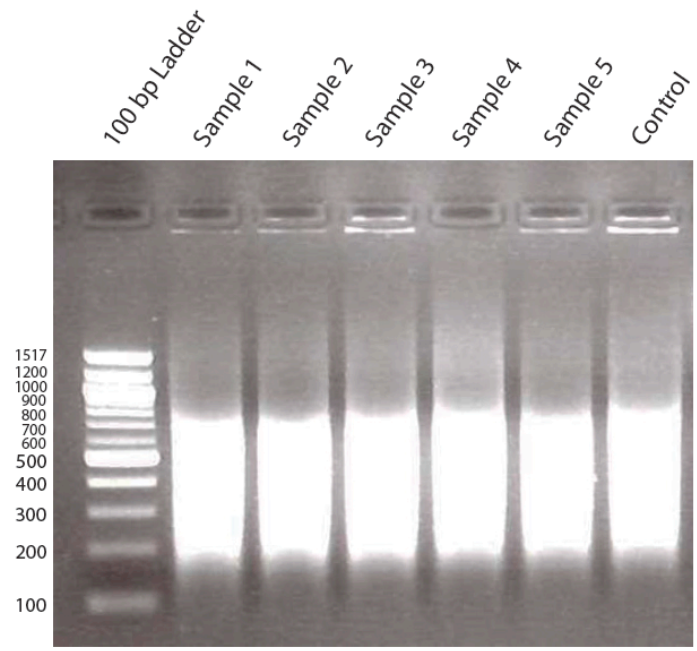

Figure_8: Agarose gel electrophoresis (1.5 %) of WGA DNA. 10% of the reactions were applied to the gel. Sample 1-5: 5 reactions of WGA were run in parallel Control; amplified DNA. A bp ladder (100 bp ladder from New England Biolabs, USA) was use to indicate size.

Presentation of methylation status between patients and controls by comparing results obtained from microarray (example from the *FLCN*)

Processing of the Human DNA Methylation 2.1M Deluxe Promoter array data generated results that could be visualized in the software SingleMap provided by NimbleGen Roche, Inc. Signal Map enables us to visualize data organized into panes and tracks, and thereby identify peak correlations between our data and annotated tracks like transcription start sites and CpG-islands. Analysis with SingleMap was performed on many of the identified regions, and to provide an example, the panels in figure_9 show the methylation differences between one patient and one control across a selected region of the FLCN gene. In the upper panel, nucleotide position on chromosome 17 is indicated by 1000 bp intervals. The next panel shows the annotated data for CpG-islands in this part of the FLCN gene. The green bar below indicates a CpG-island that is located around 17,065,700. In the middle and lower panel, the pink lines show the number of hits in the array hybridization for the patient and blue lines show the number of hits for the control. The area found differentially methylated between patients and controls after biostatistical calculations are marked with a red box. From this figure we can see that there is a clear difference in hits in the selected region between one patient and one control, and thus a difference in methylation status. It also shows us that this area is located in vicinity of a CpG-island, in a so-called CpG-island shore (Irizarry, Ladd-Acosta et al. 2009). As the methylation status of CpG-island shores is strongly related to gene expression, the region is potentially very interesting. The drawback when it comes to SignalMap as a tool to analyze the data provided from NimbleGen Roche, is that it is not possible to compare all patients and controls simultaneously, and therefore not possible to calculate the statistical difference in methylation of the patients and control as groups. The CpG-island is situated in the region from 17,065,424 to 17,065,656. This correlates with the data from the UCSC genome browser.

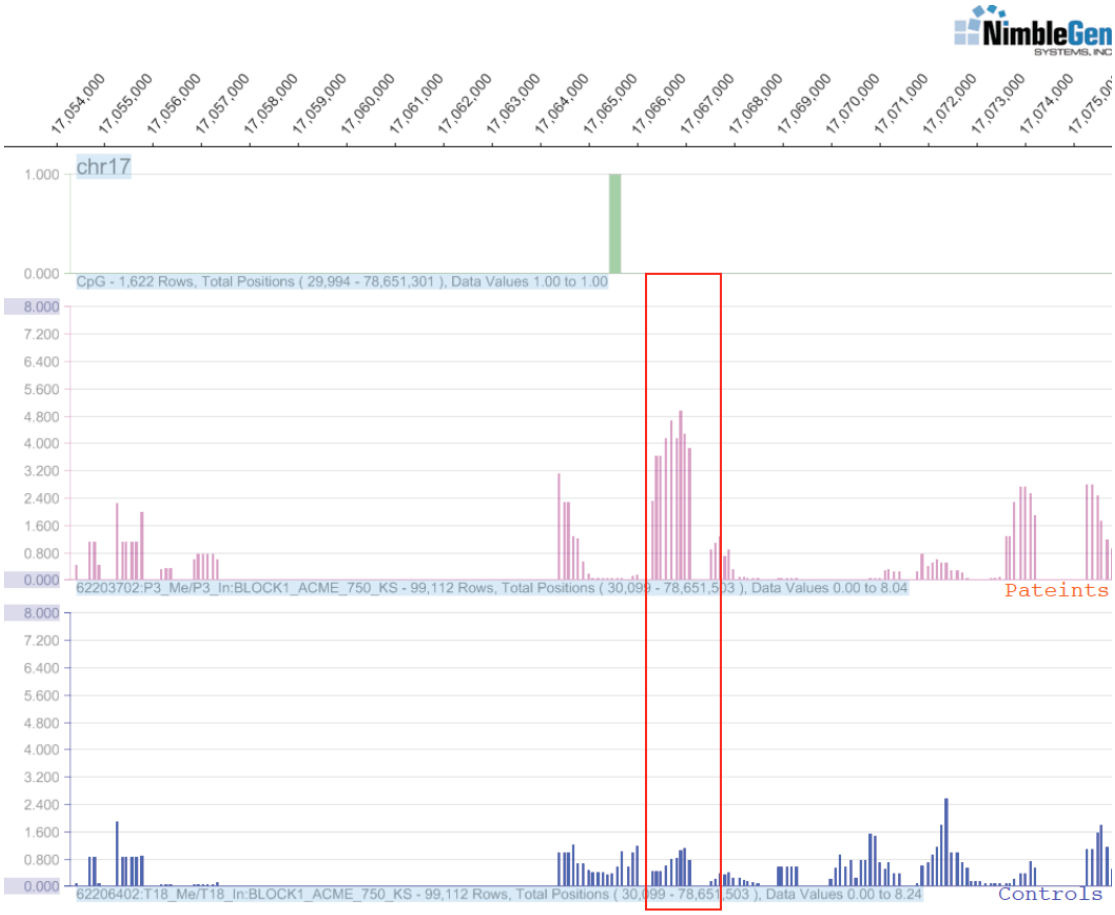

Figure_9: Statistical analysis of DNA methylation status for the genomic region corresponding to FLCN gene by using the Human DNA Methylation 2.1M Deluxe Promoter array and visualized in the software SignalMap supplied by NimbleGen Roche, Inc. The numbers on top indicate the base pair position of the FLCN gene on chromosome 17 (http://genome.ucsc.edu/). The CGI in exon-8 is shown in green in the upper panel. In middle and lower panel, the pink and blue vertical lines illustrate the number of hits in the array hybridization, for patients and controls, respectively. The region highlighted by the red box (1434 bp, from position 17,067,730 to 17,066,296) was differentially methylated in all patients and all controls.

Functional assessment of MSP primers for *FLCN*

An intragenic region in the FLCN gene (*FLCN*) was found to be hypermethylated in all AAD patients compared to controls. The *FLCN* encodes folliculin, a protein known as a co-player in apoptosis and down regulates the immune response. Moreover, the finding that the differently methylated region was localized to a CpG-island shore, made this as interesting region to analyse further. The *FLCN* contains 14 exons, and is located on the negative strand of chromosome 17, which is in the Smith-Magenis syndrome region (location: 17p11.2). Exons 4 to 14 contain the coding sequence and exons 1 to 3 are non-coding (figure_10A). According to the UCSC genome browser (http://genome.ucsc.edu/), *FLCN* contains two CGIs; one is located in 640 bp downstream of the region that was hypermethylated in patients (CpGI-2; 17,065,424 to 17,065,656 bp, 233 bp long) and the other is located to the promoter region of the gene (CpGI-1; 17,080,843 to 17,081,805, 963 bp long)(figure_10A). For all genes analysed, CpG-islands were predicted by searching the sequence one base at a time, scoring each dinucleotide (+17 for CG and -1 for others) to get maximally scoring segments, which are then evaluated with the definition of Gardiner-Garden, 1987 (Gardiner-Garden and Frommer 1987).

Interestingly, the region that was identified as hypermethylated in patients compared to controls in the MeDIP-chip, is located within 640 bp upstream of the CGI in exon 7 (indicated by grey bars in figure_10A). CpG rich regions that are located in the vicinity of a CGI are referred to as a 'shores'. CGI shores are known to be particularly dynamic with regard to methylation status and are often modified in disease (Irizarry, Ladd-Acosta et al. 2009). The identified region contains 34 CpG sites, but do not form a CGI according to the settings stated above. MSP primers were designed as outlined in figure_10C, covering six CpG sites in the amplicon. As shown in figure_10D, the methylated primers specifically amplified a product of 181 bp when methylated DNA was used as template, whereas the unmethylated primers only produce a product from unmethylated DNA (figure_10E). This result demonstrates that these primer sets designed for the FLCN gene specifically hybridize to fully methylated or unmethylated DNA.

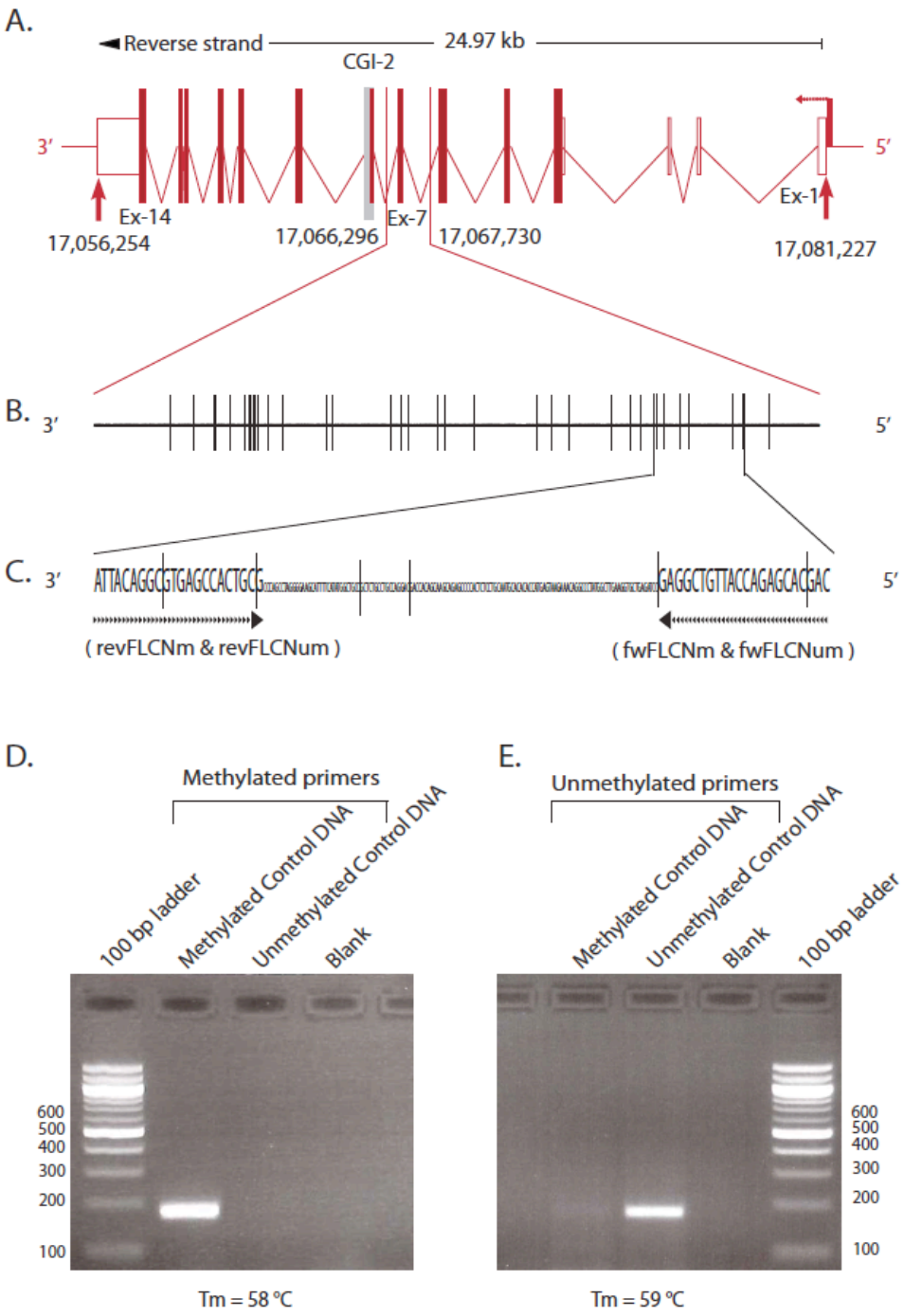

Figure_10: MSP primer pair screening for *FLCN*.

A: Schematic presentation of the *FLCN* where exons 1-14 indicated by red bars. The gene is 24.97 kb long; spanning from position 17,081,227 to 17,056,254 on chromosome 17. The identified CGI is indicated by a grey bar. The promoter is indicated by transcription start side (TSS) and located between position 17,081,995 and 17,080,614. TSS is indicated by a broken arrow; the region identified as hypermethylated in AAD patients (spanning from nucleotide position 17,067,730 to 17,066,296) is indicated by bordering with red lines in A, and highlighted with each CpG site illustrated by a vertical line in B. C: The MSP-amplified region is highlighted with the amplified sequence and indicated primers binding sites (upper case) with covered CpG sites shown. D, E: Agarose gel electrophoresis (2.5%) of PCR products (181 bp) generated by methylated primers (D) and unmethylated primers (E). A 100 bp ladder (New England Biolabs, USA) was use to indicate size.

Functional assessment of MSP primers for *SLC30A10*

The promoter region of the gene encoding SLC30A10 (solute carrier family 30 member 10) was hypermethylated in AAD patients. SLC30A10 is a Zn-transporter that has been associated with the development of autoimmune Parkinson's disease (Hamza, Zabetian et al. 2010). The gene contains 4 exons, and is located on the negative strand of chromosome 1 (location: 1q41). Exon 3 and 4 are coding sequence whereas exons 1 to 2 are non-coding (figure_11A). According to the UCSC genome browser (http://genome.ucsc.edu/), the *SLC30A10* contains one CGI; covering the gene regulatory region and non-coding first exon completely.

Interestingly, the similarly to *FLCN,* the region identified as hypermethylated in patients in *SLC30A10,* is also located a putative CGI shore (within 175 bp upstream of the CGI) (figure_11A). The identified region contains 15 CpG sites, but do not form a CGI according to the settings stated above (figure_11C). MSP primers were designed as outlined in figure_11C, covering seven CpG sites in the amplicon. As shown in figure_11D, the methylated primers specifically amplified a product of 170 bp when methylated DNA was used as template, whereas the unmethylated primers only produce a product from unmethylated DNA (figure_11E). This result demonstrates that these primer sets designed for the *SLC30A10* specifically hybridize to fully methylated or demethylated DNA.

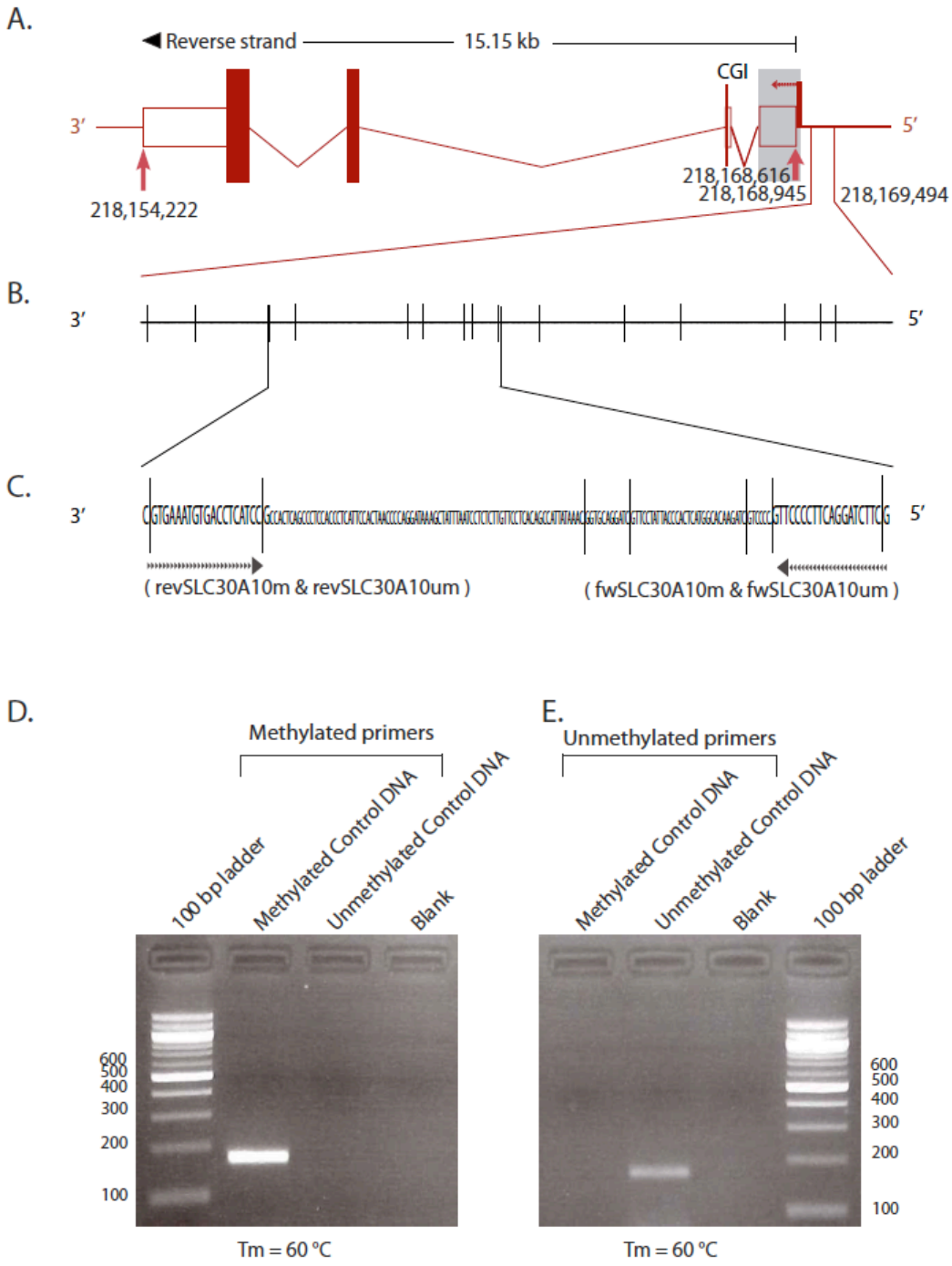

Figure_11: MSP primer pair screening for *SLC30A10*.

A: Schematic presentation of *SLC30A10* with exons 1-4 indicated by red bars. The gene is 15.15 kb; and located at position 218,168,616 to 218,154,222 on chromosome 1. The transcription start site is indicated by a broken arrow and the identified CGI by a grey bar. The region identified as hypermethylated in AAD patients (spanning from nucleotide position 218,169,494 to 218,168,945) is located 329 bp upstream of first exon and is indicated by bordering with red lines in A. This region is highlighted with each CpG site illustrated by a vertical line in B. C: The MSP-amplified region is highlighted with the amplified sequence and indicated primers binding sites (upper case) with covered CpG sites shown. D, E: Agarose gel electrophoresis (2.5%) of PCR products (170 bp) generated by methylated primers (D) and unmethylated primers (E). A 100 bp ladder (New England Biolabs, USA) was use to indicate size.

Functional assessment of MSP primers for *HDAC4*

An intragenic region was found to be hypermethylated in the gene encoding histone deacetylase 4 (HDAC4) in AAD patients compared to controls. As the name indicates, HDAC4 deacetylates histones, which generally leads to a closed chromatin structure and transcriptional repression. However, the major reason for analysing this gene further was the well-established association of HDACs in autoimmunity (Brooks, Le Dantec et al. 2010). The gene contains 27 exons, and is located to the negative strand of chromosome 2 (location: 2q37.3). Exons 2 to 27 are coding sequence and exon 1 is non-coding (figure_12A). According to the UCSC genome browser (http://genome.ucsc.edu/), the *HDAC4* contains fifteen CGIs.

The region that was identified as hypermethylated in patients is located in intron/exon as 1-2/2 (figure_12A) and therefore interesting since first exon is potentially important for transcription initiation. The identified region contains 45 CpG sites (figure_12B), but although the CpG site density is high it is not defined as a CGI according to the settings stated above. MSP primers were designed as outlined in figure_12C, covering eight CpG sites in the amplicon. As shown in figure_12D, the methylated primers specifically amplified a product of 112 bp when methylated DNA was used as template, whereas the unmethylated primers only produce a product from unmethylated DNA (figure_12E). This result demonstrates that these primer sets designed for the HDAC4 gene specifically hybridize to fully methylated or unmethylated DNA.

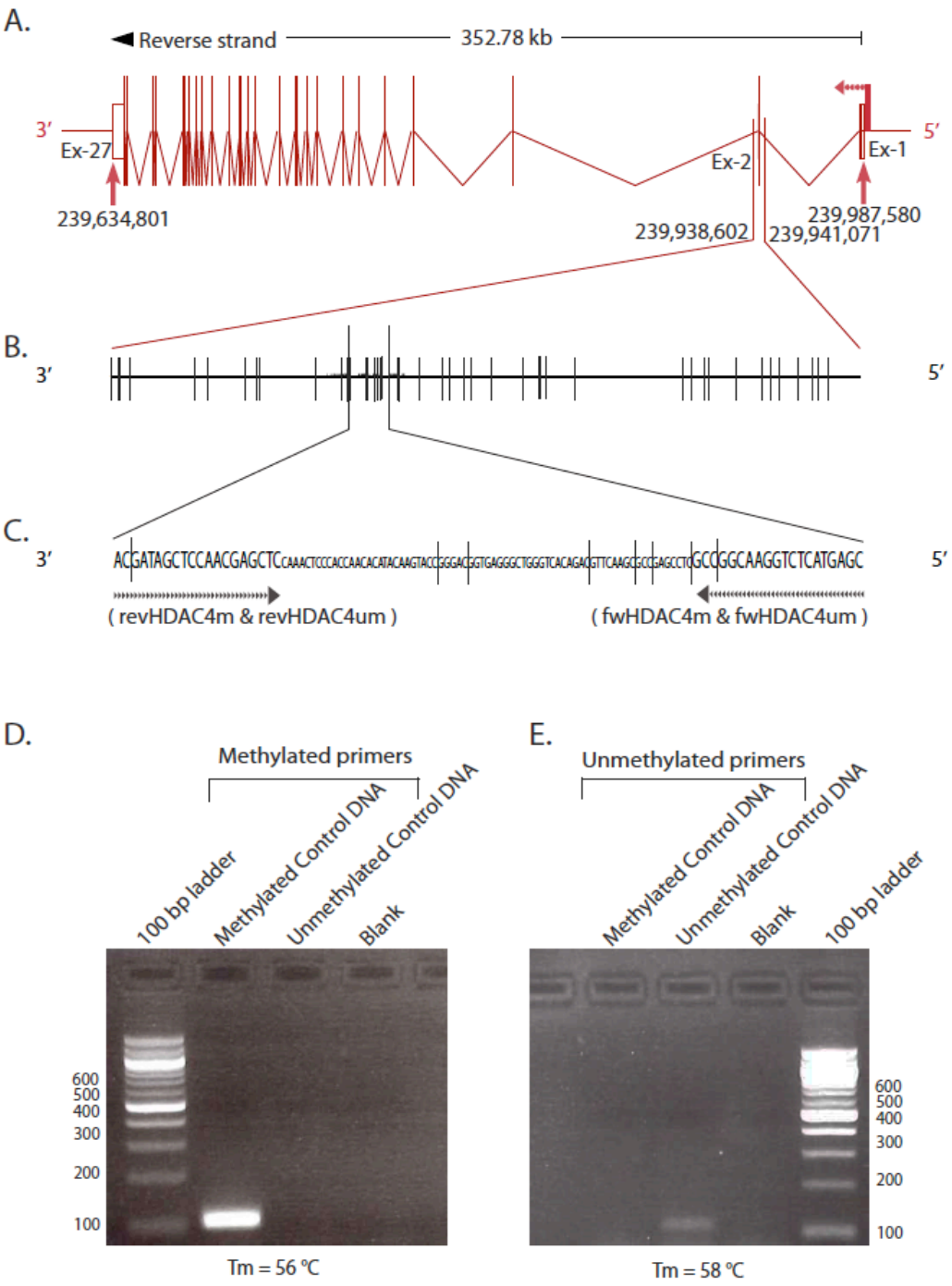

Figure_12: MSP primer pair screening for *HDAC4*.

A: Schematic presentation of the HDAC4 gene with exons 1-27 indicated by red bars. The gene is 352.78 kb and located at position 239,987,580 to 239,634,801 on chromosome 2. Regulatory region featured from 239,988,808 bp to 239,987,567 bp. The transcriptional start site is indicated by a broken arrow. The region identified as hypermethylated in AAD patients (spanning from nucleotide position 239,941,071 to 239,938,602) is indicated by bordering with red lines in A. This region is highlighted with each CpG site illustrated by a vertical line in B. C: The MSP-amplified region is highlighted with the amplified sequence and indicated primers binding sites (upper case) with covered CpG sites shown. D, E: Agarose gel electrophoresis (2.5%) of PCR products generated (112 bp) by methylated primers (D) and unmethylated primers (E). A 100 bp ladder (New England Biolabs, USA) was use to indicate size.

Functional assessment of MSP primers for *RCC2*

An intragenic region in the gene encoding regulator of chromosome condensation 2 (RCC2) was found to be hypermethylated in patients with AAD compared to controls. RCC2 protein is required in normal cell division and has not been associated with autoimmunity but the abnormal methylation pattern identified with MeDIP-chip was highly methylated in patients compare to control. The fact that this gene harbours three CGIs ensured me to go further with MSP analysis. The gene contains 13 exons and is located to the negative strand of chromosome 1 (location: 1p36.13). Exons 2 to 13 are known as protein coding exons and exon 1 is non-coding (figure_13A). According to the UCSC genome browser (http://genome.ucsc.edu/), the gene contains three CGIs.

The region identified as hypermethylated in patients compared to controls is located in exon 8-11 (figure_13A). The identified region contains 45 CpG sites (figure_13B) but do not form a CGI according to the settings stated above. MSP primers were designed as outlined in figure_13C, covering six CpG sites in the amplicon. As shown in figure_13D, the methylated primers specifically amplify a product of 121 bp when methylated DNA was used as template, whereas the unmethylated primers produce a product of the same size from unmethylated DNA (figure_13E). For both methylated and unmethylated DNA, an unspecific band appeared with the unmethylated (figure_13E). This is the reason of unmethylated primers trends to bind unspecifically. This result demonstrates that these primer sets designed for the RCC2 gene specifically hybridize to fully methylated or unmethylated DNA.

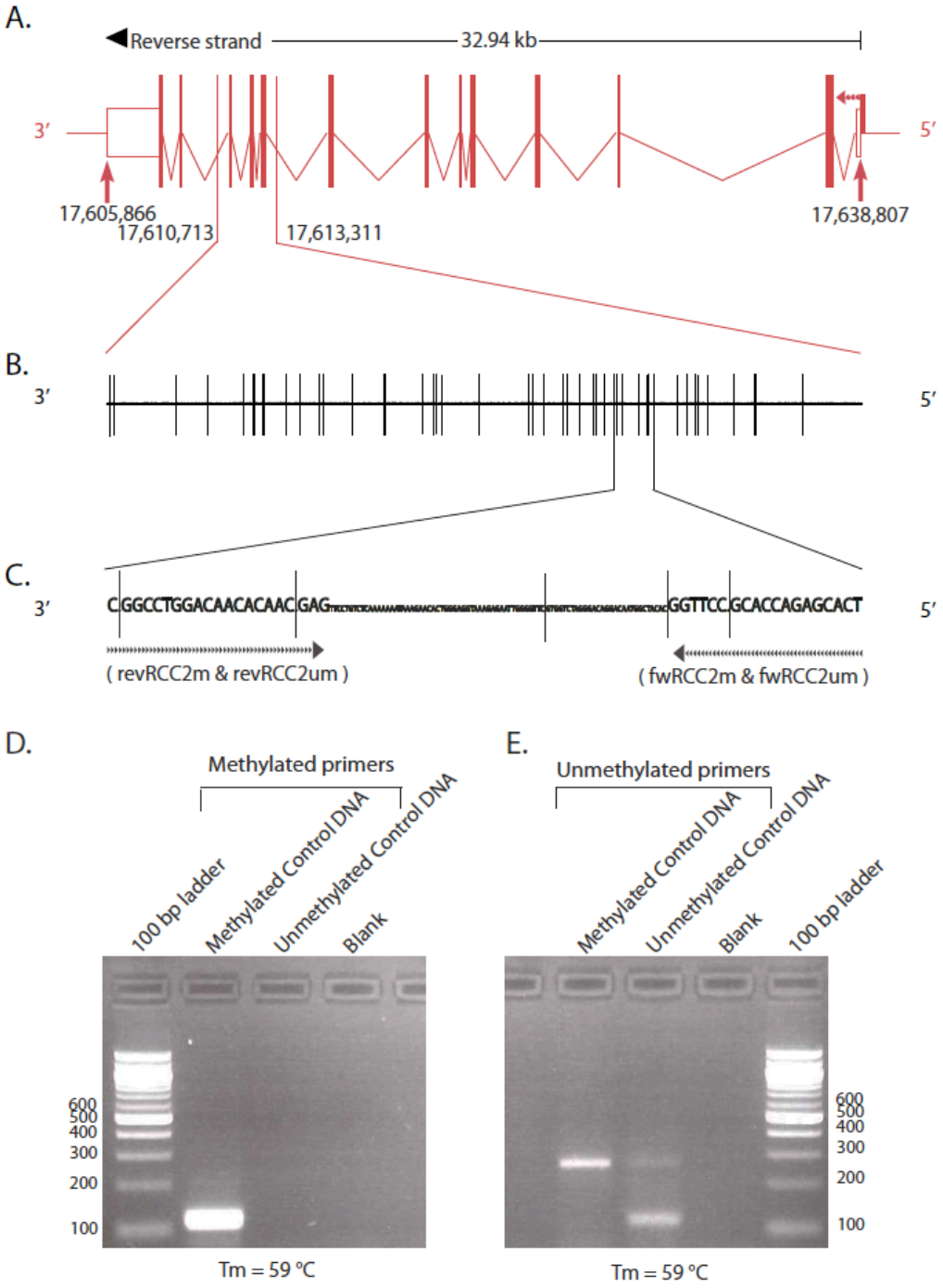

Figure_13: MSP primer pair screening for *RCC2*.

A: Schematic presentation of the RCC2 gene with exons 1-13 indicated by red bars. The gene is 52.94 kb, spanning nucleotide position 17,638,807 to 17,605,866 on chromosome 1. The promoter is located at 17,639,023 to 17,638,675. The transcriptional start site is indicated by a broken arrow. The region identified as hypermethylated in AAD patients (spanning nucleotide position 17,610,713 to 17,613,311) is indicated by bordering with red lines in A. This region is highlighted with each CpG site illustrated by a vertical line in B. C: The MSP-amplified region is highlighted with the amplified sequence and indicated primers binding sites (upper case) with covered CpG sites shown. D, E: Agarose gel electrophoresis (2.5%) of PCR products generated (121 bp) by methylated primers (D) and unmethylated primers (E). A 100 bp ladder (New England Biolabs, USA) was use to indicate size.

Functional assessment of MSP primers for *GRIN2B*

A region localized to an intronic CGI in the gene encoding N-methyl-D-aspartate receptor subunit 2B (GRIN2B) was found to be hypermethylated in AAD patients compared to controls. GRIN2B is important for memory and learning processing, and is associated with autoimmune schizophrenia disorder responses (Carter 2011). *GRIN2B* contains 13 exons, and is located to the negative strand of chromosome 12 (location: 12p13.1). All exons contain coding sequence (figure_14A). According to the UCSC genome browser (http://genome.ucsc.edu/), the *GRIN2B* gene contains one CGI; located in exon 13 (spanning nucleotide position 13,608,301 to 13,607,117; 1185 bp long) (figure_14A).

Interestingly, the region that was identified as hypermethylated in patients compared to controls in the MeDIP-chip, is located within a CGI in exon 13 (figure_14A). The majority of CGIs are kept unmethylated, and only around 5 % of CGIs are differentially methylated. The identified region contains 58 CpG sites and this is a CGI according to the settings stated above (figure_14C). MSP primers were designed as outlined in figure_14C, covering thirteen CpG sites in the amplicon. As shown in figure_14D, the methylated primers specifically amplified a product of 170 bp when methylated DNA was used as template, whereas the unmethylated primers only produce a product from unmethylated DNA (figure_14E). This result demonstrates that these primer sets designed for the GRIN2B gene specifically hybridize to fully methylated or unmethylated DNA.

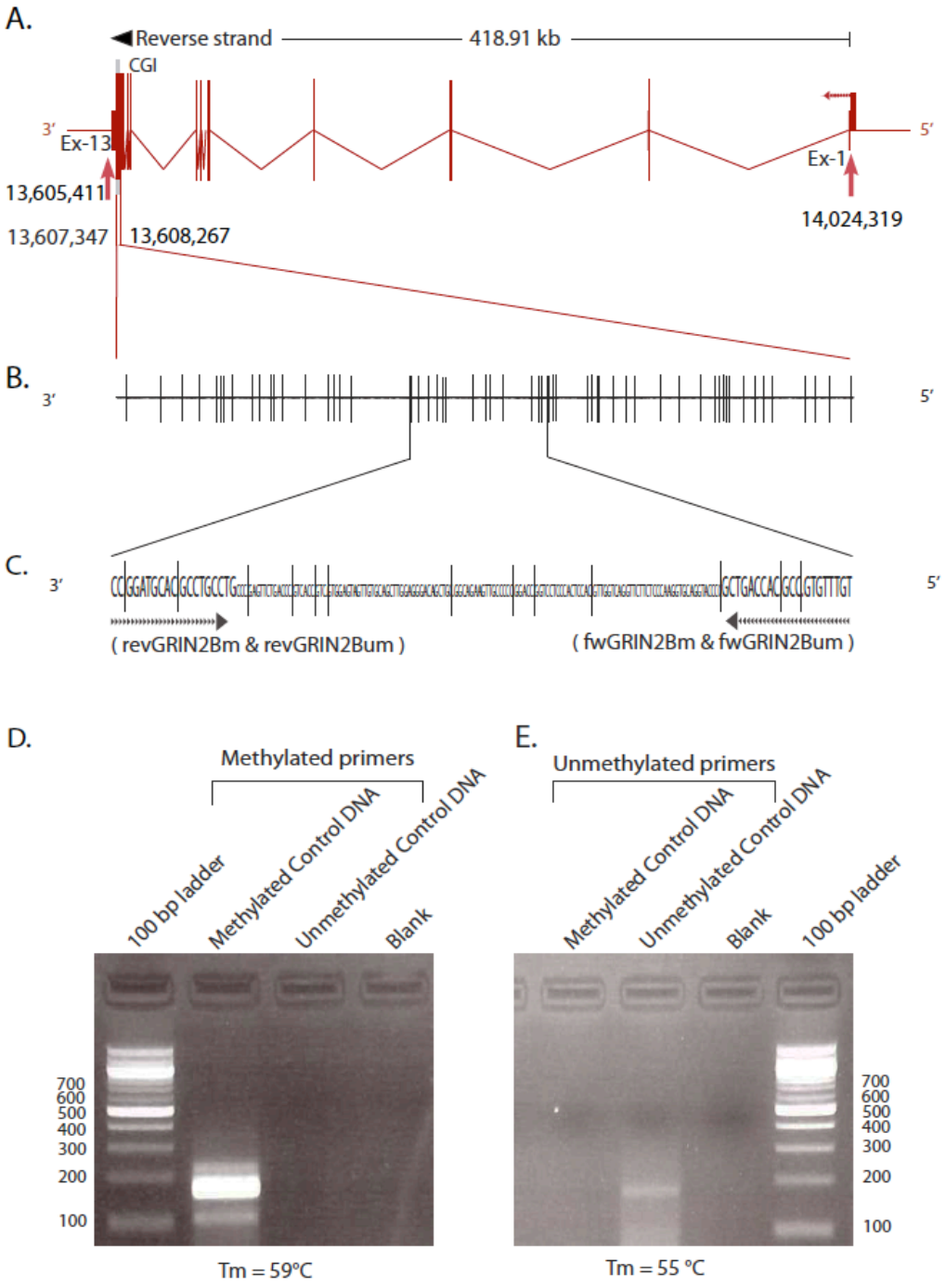

Figure_14: MSP primer pair screening for *GRIN2B*.

A: Schematic presentation of the GRIN2B gene with exons 1-13 indicated by red bars. The gene is located to chromosome 12, spans 418.91 kb (nucleotide positions 14,024,319 to 13,605,411). The transcriptional start site is indicated by a broken arrow. The region identified as hypermethylated in AAD patients (spanning nucleotide position 13,608,267 bp to 13,607,348 bp) is indicated by bordering red lines in A. This region is highlighted with each CpG site illustrated by a vertical line in B. C: The MSP-amplified sequence region is highlighted with the amplified sequence and indicated primers binding sites (upper case) with covered CpG sites shown. D, E: Agarose gel electrophoresis (2.5%) of PCR products generated (170 bp) by methylated primers (D) and unmethylated primers (E). A 100 bp ladder (New England Biolabs, USA) was use to indicate size.

MSP to analyse the methylation status of the *FLCN* in AAD patients and controls

As shown in figure_10, the MSP primers discriminated between fully methylated or unmethylated DNA across the region of the FLCN gene that was identified as hypermethylated in AAD patients compared to controls in the MeDIP-chip dataset. To investigate whether the difference in methylation status would be evident with MSP, DNA from five patients (figure_15A-B) and five controls (figure_15C-D) where analyzed with MSP. Importantly, these patients and controls were also included in the MeDIP-chip. As expected, the methylated and unmethylated primers only amplified product from the methylated and unmethylated controls, respectively, but the unmethylated primers were less efficient than the methylated primers (figure_15). The methylated primers amplified efficiently the right product from patient DNA (figure_15A) and although MSP-products with methylated primers were also evident in the control samples (figure_15C), these bands were relatively weaker than in the patients. It is difficult to interpret the results obtained with the unmethylated primers due to the low levels of amplicon. But the difference is visible (figure_15B-D) where at least one control (C-4 in figure_15D) is presenting a very week band along with the unmethylated control DNA. It is although clearly demonstrated that MSP on DNA from patients did not generate product with unmethylated primers (figure_15B). This finding is therefore in accordance with the MeDIP-chip results, namely that this region is hypermethylated in patients.

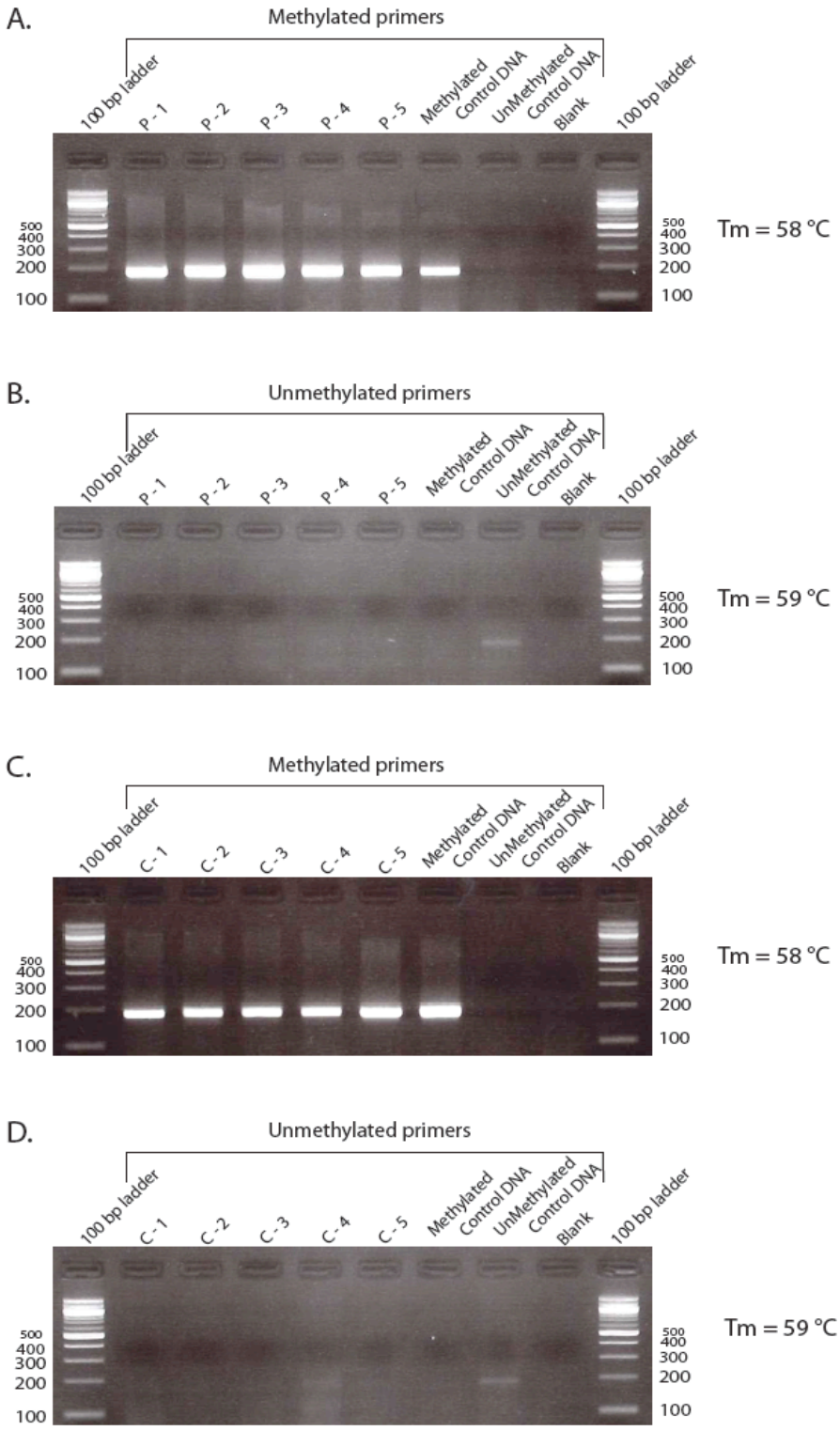

Figure_15: Methylation status of the differentially methylated region identified in the *FLCN*.

Agarose gel electrophoresis (2.5%) on MSP products obtained with methylated (A and C) and unmethylated primers (B and D) on DNA isolated from AAD patients (A and B) or control individuals (C and D). P1 to P5 are samples from patients and C1 to C5 are samples from control donors. Methylated Control DNA; fully methylated DNA, Unmethylated Control DNA; WGA amplified (unmethylated DNA), blank; no DNA. A 100 bp ladder (New England Biolabs, USA) was used as size marker.

Discussion

DNA methylation affects approximately 1% of DNA bases in the human genome and is a major epigenetic modification in respect to tissue specific gene expression (Hughes and Jones 2007). It is today well recognized that generally, hypermethylation leads to gene silencing and hypomethylation to gene expression. Thus, DNA methylation might be viewed as a controlling system for gene expression that acts independently of alternations in the DNA sequence (Umetani, de Maat et al. 2005). Since DNA methylation is reversible, there is great therapeutic interest in the process. Moreover, it is therefore also immense interest in the basic mechanisms of DNA methylation and how it contributes to diseases development. Complex diseases like cancer and autoimmune disorder are mostly polygenic, and it is also commonly believed that epigenetic mechanisms contribute as well. DNA hypermethylation, and in some cases hypomethylation, are found in some forms of cancer and autoimmune disorders (Fraga, Ballestar et al. 2005; Handel, Ebers et al. 2010; Meda, Folci et al. 2011). The human epigenome project is ongoing to map genome-wide the DNA methylation patterns of all human genes in all major tissues (http://www.epigenome.org) and will eventually provide an invaluable tool to understand the role of DNA methylation in embryonic development, physiology and disease. DNA methylation plays a regulative role in the genome rather than the only initiating gene silencing (Weber and Schubeler 2007). This is a dynamic feature where the gene expression pattern of a cell depends upon its methylation profile (Paulsen and Ferguson-Smith 2001). Overall, only around 4-8% of CGIs exhibit tissue specific methylation (Shen, Kondo et al. 2007; Irizarry, Ladd-Acosta et al. 2009; Illingworth, Gruenewald-Schneider et al. 2010). The remaining CGIs are found throughout genes associated with exons (coding and non-coding) and introns where they might also be important for gene expression by producing defective protein. DNA methylation and demethylation in the genome is established as a model for inhibition of cryptic initiation, protection against mobile elements and maintenance of genome stability (Weber and Schubeler 2007). Aberrant DNA methylation can lead to chromosomal instability which can cause mutation in gene thereby affect gene expression (Paulsen and Ferguson-Smith 2001).

Autoimmune diseases comprise a large group of systemic and organ specific disorders that together constitute a major cause of illness and death. Autoimmune diseases are typically manifested by abnormal differentiation of different subtypes of CD4+ T-cells (e.g. regulatory T-cells; T_{REG}, IL-17-producing T helper cells; Th17 and IL-22 producing T helper cells; Th22) followed by abnormal production of interleukins (Buckner 2010). The incidence ratio for autoimmune disease is strikingly higher in females, with a prevalence as high as 10:1 (Invernizzi, Pasini et al. 2009). Surprisingly, the frequency of autoimmune Addison's disease is higher in young people and predominantly in female within the age of 20-60 years. In the study that this thesis is a part of, the choice of patient group was female in the range of between 20-60 years due to the fact that most patients in the Norwegian Addison's Disease cohort are this group with in as the risk probability showed in statistics indicate (Erichsen, Lovas et al. 2009). Although DNA methylation has not previously been studied in an AAD cohort, it is established that epigenetic abnormalities are associated with autoimmune diseases. This is exemplified by studies demonstrating that changes in genome-wide T-cell DNA methylation is associated with various autoimmune diseases, and they suggest that changes in DNA methylation causes aberrant gene expression leading to loss of tolerance in CD4+T-cells (Jeffries, Dozmorov et al. 2011). This study shows that the difference between patients with autoimmune disease and healthy controls in respect to DNA methylation is cell type specific. The difference is cell type specific primarily in CD4+ T-cells for AAD. Other studies exemplified in regulatory T-cells and B cells for SLE (Jeffries, Dozmorov et al. 2011); lymphocytes and synovial fibroblast for RA (Rodrigues, Jungel et al. 2009); and lymphocytes and skin fibroblast for the patient with systemic sclerosis. Examples of organ specific autoimmune disease are type 1 diabetes, multiple sclerosis (MS), idiopathic thrombocytopenic purpura (ITP) and celiac disease (Brooks, Le Dantec et al. 2010).

Epigenetic regulation of immune regulatory genes is demonstrated in several studies. FoxP3 is a forkhead family transcription factor expressed and required for development of CD4+ regulatory T-cells, therefore, involved in autoimmune reaction (Polansky, Kretschmer et al. 2008). Mutations of FoxP3 lead to deficiency of regulatory T-cells and development of autoimmunity appear most likely due to lack of negative selection (Floess, Freyer et al. 2007). Moreover, the expression of *FoxP3* is methylation sensitive and the proximal promoter methylation status revealed the significant difference in other autoimmune disorder (Li, Zhao et al. 2011). Thus, FoxP3 is a candidate gene for its functional importance in the development of autoimmune disease. Another candidate gene for autoimmune disease is AIRE

(autoimmune regulator). This is a transcription factor is involved in central tolerance and clonal deletion of self-reactive T-cells. DNA methylation in CpG sites of the *AIRE* promoter controls its tissue specific expression (Kont, Murumagi et al. 2011). For an instance, DNA methylation of histone 3 affects the expression of *AIRE* (Javierre, Esteller et al. 2008).

There are several methods to analyze DNA methylation status. Bisulfite conversion followed by PCR and sequencing (BSP) is one the mostly used method, and often called the gold standard in monitoring DNA methylation as it allows for single-base pair resolution maps. Sodium bisulfite, which is a mutagen in the environment, leads to determination of cytosine into uracil. The major advantages of the bisulfite method are accurate display of 5-methylcytosine and the capacity to generate sequence data for individual CpG sites and DNA strands (Frommer, McDonald et al. 1992). The established BSP protocol in Marit Bakke lab uses nested PCR instead of traditional PCR after bisulfite conversion because the bisulfite treated DNA is fragile and difficult to amplify. Nested PCR enable us to amplify the region of interest without requiring too much template and reduce nonspecific amplification. BSP was used initially in this master thesis to assess DNA methylation differences between AAD patients compared to control blood donors across one genomic region that were identified in the MeDIP-chip as differentially methylated in patients and controls (data not shown). The gene analyzed with this method was FoxP3, as AAD patients where hypermethylated compared to controls in the promoter region of this gene. The BSP analysis of *FoxP3* revealed no differences in the methylation status between patients and controls (figure_7). The main drawback with the BSP approach in this context is the very low throughput. Only a very limited amount of individuals and clones can be analyzed at a time, and thus BSP is not suitable as a screening method. At present, therefore, no conclusion can be drawn from the BSP analysis of the FoxP3 gene due to the few clones analyzed from only two individuals. Because of these limitations of BSP, we decided to establish MSP in the lab; partly to verify the MeDIP-chip results, but also to obtain a tool to screen other cohorts across interesting regions.

MSP is a method in which the amplification of a genomic region depends on the methylation status of the sequence covered by the primers (Rand, Qu et al. 2002). MSP is probably most sensitive non-quantitative method due to its capability to detect 0.1% methylation or less which can cover any block of CpG sites (Rand, Qu et al. 2002; Kristensen, Mikeska et al. 2008). This method can be made quantitative by either labeling the primers with fluorofores

or by combining the MSP primers with an internal labeled fluorescent probe. The quantitative version of MSP is also known as MethyLight, and allows for moderate-throughput quantitative methylation profiling of a group of gene (Zuo, Tycko et al. 2009). The main drawback of MSP is that it can be very challenging to design primer sets that will work well for both unmethylated and methylated sites. The software Methyl Express was used to design the primers, but still this part is very time consuming. Many primer sets were evaluated in silico, and for most genes several sets of primers were also tested in the lab. It was observed that the software often recommended an annealing temperature 3-5ºC higher that what was found to be optimal for the PCR. My observations also suggested that the unmethylated primer pairs worked better at higher melting temperatures than the methylated primer pairs, and different annealing temperature were therefore often used for the methyalated and unmethylated primers for a specific region. Another problem with all bisulfite-based methods is incomplete conversion unmethylated cytosine to uracil. This fact may lead to that the primer sets do not hybridize well to the region of interest and inhibit specific primer binding. To overcome this challenge with MSP, controls in the form of completely methylated and unmethylated DNA are necessary. Completely methylated control DNA is available commercially, but the completely unmethylated control DNA purchased from New England Biolabs was not reliable. Demethylated DNA was therefore prepared by whole genome amplification (WGA) of DNA isolated from whole blood. In WGA the DNA is amplified without any addition of the methyl group to the newly formed DNA molecules due to lack of DNMTs and the methyl source s-adenosyl methionine (SAM) in the reaction. (Kristensen, Mikeska et al. 2008).

Though MSP is a highly sensitive and virtually capable to recognize any block of differentially methylated CpG sites (Umetani, de Maat et al. 2005), it need optimization of temperature and cycle alongside proper methylated and unmethylated control DNA. The temperature when preparing the MSP samples is critical, and if the sample with both template and polymerase is stored at room temperature GoTaq polymerases could facilitate 3' mismatch. The samples should therefore at all times be handled on ice during preparation. This is especially important because bisulfite converted DNA is the template, due to higher chance of default template-DNA binding and primer-dimer formation. The choice of DNA polymerase enzyme and optimization of its activation temperature are thus a most critical step to successful MSP. The use of hot start DNA polymerase or DNA polymerase addition after initiation step could be ways to overcome this critical situation. Inappropriate melting

temperature can cause primer binding to wrong places and this can give a smear in the agarose gel. A second step that should be optimized is the DNA concentration used in the reaction. DNA concentration should be fixed for both positive and negative control DNA (methylated and unmethylated DNA, respectively) as well as the patient/control sample during the primer screening.

MeDIP and subsequent hybridization to DNA tilling arrays, followed by statistical analyses identified genomic regions that where differently methylated in all patients compared to all controls (appendix 1 page 68-70). In characterization of genes related to autoimmune disease it is not essential that the genes are " immune response" gene. It is established Chen et al. that the genes also could be involved in apoptosis, cell cycle progression, cell differentiation and migration (Maas, Chan et al. 2002). The criteria mentioned in the results section were used as basis to select genes for MSP analysis. The following genes were selected because of their relation to autoimmune diseases along with their interesting DNA methylation pattern and their possible connection in AAD.

FLCN (coding for protein folliculin): The protein is characterized as a possible tumor suppressor involved in apoptosis by two different signalling pathways (Vocke, Yang et al. 2005; Hong, Oh et al. 2010; Hudon, Sabourin et al. 2010; Cash, Gruber et al. 2011). It is involved in energy and/or nutrient sensing through mTOR signaling pathways (Hartman, Nicolas et al. 2009; Lim, Fujikane et al. 2012). This protein has not been directly linked to autoimmunity before, but because of the role of its interacting partner protein Bim in the termination of immune response it was included as a interesting gene investigate further with the MSP analysis. Moreover, the region identified as hypermethylated in patients was localized to a CGI shore, and completely covered a protein coding exon (figure_10A). CGI shores are of particular interest as they are often present in gene regulatory regions and are often differently methylated between tissues (Irizarry, Ladd-Acosta et al. 2009).

SLC30A10 (Zn transporter): This gene is highly expressed in the liver and has an important function in zinc and manganese transport. Mutations in this gene are recognized in autoimmune Parkinson's disease development (Hamza, Zabetian et al. 2010; Tuschl, Clayton et al. 2012). The gene-encoded protein, which is belongs to large family of membrane transporters is involved in effluxion of divalent cations from the cytosol. Depletion of

SLC3OA10 in liver is responsible for the development of autoimmune Parkinson's disease (Quadri, Federico et al. 2012).

HDAC4 (Histone deacetylase 4): The involvement of HDACs in autoimmunity is well established where inhibition of histone deactylase can increase *FoxP3* expression and suppressive function of T_{REG} cells (Tao, de Zoeten et al. 2007). HDAC4 is expressed in a tissue-specific pattern and mainly expressed in $_{TREG}$ cells (Lal and Bromberg 2009). This gene interacts with and repress MADS-box MEF2 transcription factor and therefore also repress T-cells stimulation (Potthoff and Olson 2007). MEF2 is a transcription factor involved in multiple signalling pathways and is also required for B-cells proliferation (Wilker, Kohyama et al. 2008). The covering area (second but first protein coding exon) has a high density of CpG sites and altogether this indicated the possibility of transcriptional regulation by DNA methylation.

RCC2 (regulator of chromosome condensation 2): This protein is required completion of mitosis and cytokinesis. It may also function as a guanine nucleotide exchange factor for the small GTPase RAC1 (Grigera, Ma et al. 2012). Though the gene has not been reported to be involved in the development of autoimmunity, the methylation pattern identified and the amount of hits in the array made this gene potentially interesting. The hypothesized role of DNA methylation in the gene might be linked to, inhibition of mitosis and cytokinesis.

GRIN2B (N-methyl-D-aspartate receptor subunit 2B): N-methyl-D-aspartate (NMDA) receptors are a class of ionotropic glutamate receptors mainly known as neuropsychiatric factors. The genes encoding these proteins have been associated with schizophrenia, a pathogenic autoimmune disease (Carter 2011). GRIN2B is a part of a NMDA receptor channel which has been shown to be involved in long-term potentiating, an activity-dependent increase in the efficiency of synaptic transmission thought to underline certain kinds of memory and learning (Dorval, Wigg et al. 2007). Interestingly, the only CpG-island present in this gene, fully covers the region that was identified as hypermethylated in controls. This information insinuates that transcriptional regulation of the gene could be governed by DNA methylation.

Due to time limitations, MSP was only carried out across *FLCN* on patient DNA. As mentioned above it became evident after this analysis (figure_15) that even though MSP can clearly distinguish between completely methylated or unmethylated DNA, this method is probably not sensitive enough to discriminate between individuals with less robust differences in methylation status. Q-MSP, or MethyLight as described above, will most likely be required to determine the methylation differences between patients and controls across the different genomic regions. However, the MSP-results presented in figure_15, still indicates the same results as the array, namely that the identified region in FLCN is hypermethylated in AAD patients compared to controls. It is expected that this would lead to decreased FLCN expression in AAD patients, but this remains to be tested experimentally. The skin pigmentation observed in AAD patients develops as a consequense of interuption of feedback inhibition from the adrenal and the hypothalamus and anterior pituitary gland. The disturbance leads to melanogenesis by melanocyte stimulating hormone secretion coupled with corticotropin (Burk, Ciocca et al. 2008) (figure_16A). Interestingly, the potential repressed expression of FLCN in AAD patients indicate a possible alternative mechanism for pigmentation in AAD patients (figure_16). This hypothetical model suggests that under expression of FLCN due to increased DNA methylation, a factor called of TFE3 will be induced (Hong, Oh et al. 2010). Induction of TFE3 overexpression stimulates lysosomal biogenesis. Thereon, an increased level of lysosomal biogenesis adds up to melanosome biogenesis and causes pigmentation in different organs. It should be mentioned that TFE3 is one among four members of the MiT/TFE transcription factor subfamily that is important for the expression of genes that encode lysosomal proteins such as melanin (Sardiello, Palmieri et al. 2009).

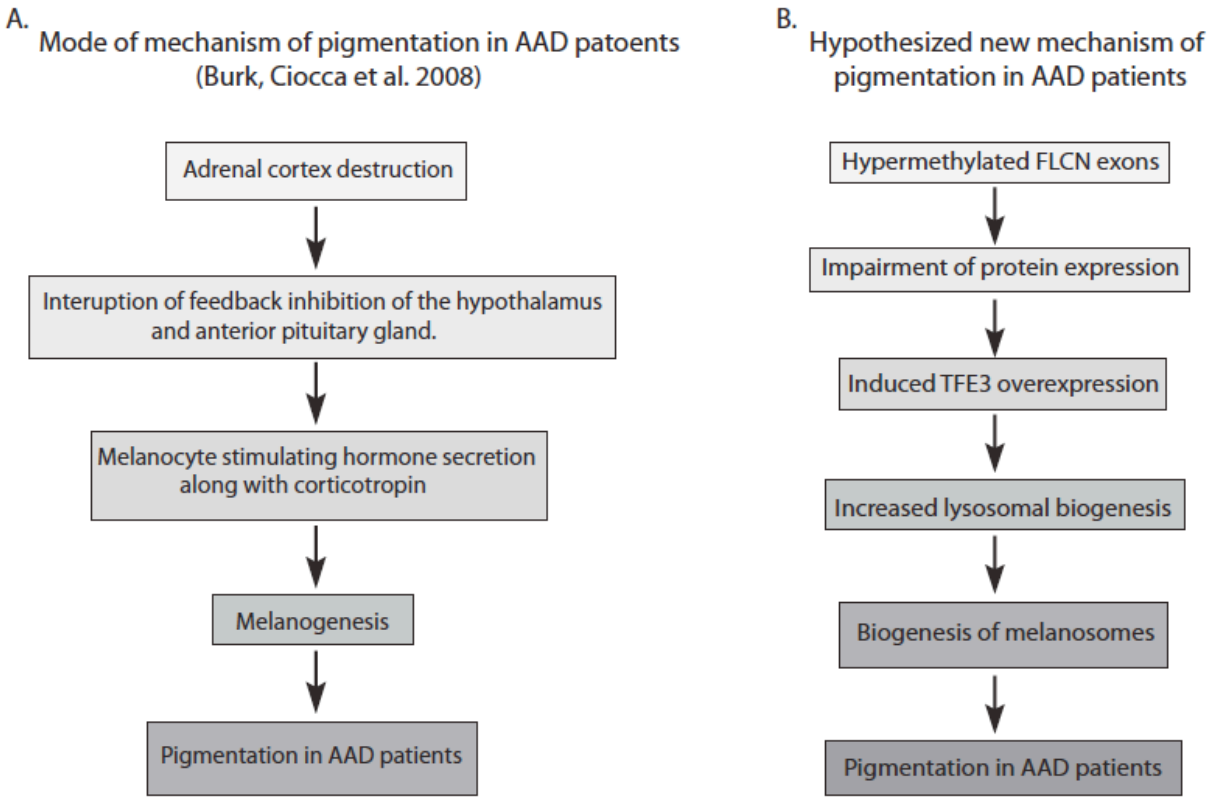

Figure_16: Proposed mechanism of hypermethylated FLCN gene in clinical manifestation by producing pigmentation for AAD patients. A: The established pathway leading to hyperpigmentation of AAD patients (Burk, Ciocca et al. 2008). B: A hypothetical alternative pathway for hyperpigmentation in AAD patients involving FLCN and TFE3.

Another interesting link between FLCN and AAD is proposed based on the direct involvement of FLCN gene on the development of autoimmunity by apoptosis (figure_17). An important regulator of apoptosis is the pro-apoptotic gene BH3-only pro-apoptotic Bcl-2 family member, commonly known as Bim. It is reported that FLCN gene expression can affect on Bim expression in the TGF-ß signalling pathway (Hong, Oh et al. 2010). The association between FLCN and Bim, as well as the individual function of Bim in apoptosis is regulated by FLCN expression via a positive feedback mechanism (Hong, Oh et al. 2010). The role of Bim in termination of immune response is to repress activated T-cells, as demonstrated in several studies (Pellegrini, Belz et al. 2003). The termination process requires Bim for the death of activated T-cells by apoptosis (Bouillet, Purton et al. 2002). FNIPL (Folliculin Interacting Protein 1-like) and FNIP2 (Folliculin Interacting Protein 2) are reported as interacting partners of FLCN (Hasumi, Baba et al. 2008). FNIP2 and FNIPL, as well as FNIP1 (Folliculin Interacting Protein 1) can interact with AMPK (5' AMP-Activated Protein Kinase) (Hardie 2004). Through the AMPK signalling pathway, a complex composed

of MAPO1 (O(6)-methylguanine-Induced Apoptosis 1), FLCN and AMPK is involved in the induction of apoptosis (Lim, Fujikane et al. 2012). On the other hand, the gene has a potential function in reducing nutrient supply for cell growth and survival maintained by mTOR signalling, leading to apoptosis (Hartman, Nicolas et al. 2009) (figure_17A), and might be the nutrient supplier for auto reactive T-cells populations in AAD patients (figure_17B). When it comes to Bim function in apoptosis and termination of immune response, the proposed hypothesis is presented in figure_17 the diagram below where the function of hypermethylated FLCN have described in the development of autoimmunity (figure_17B). Overall, the hypothesis annotated the FLCN gene in the development of autoimmunity of AAD patients due to lack of apoptosis of negatively selected auto reactive T-cells.

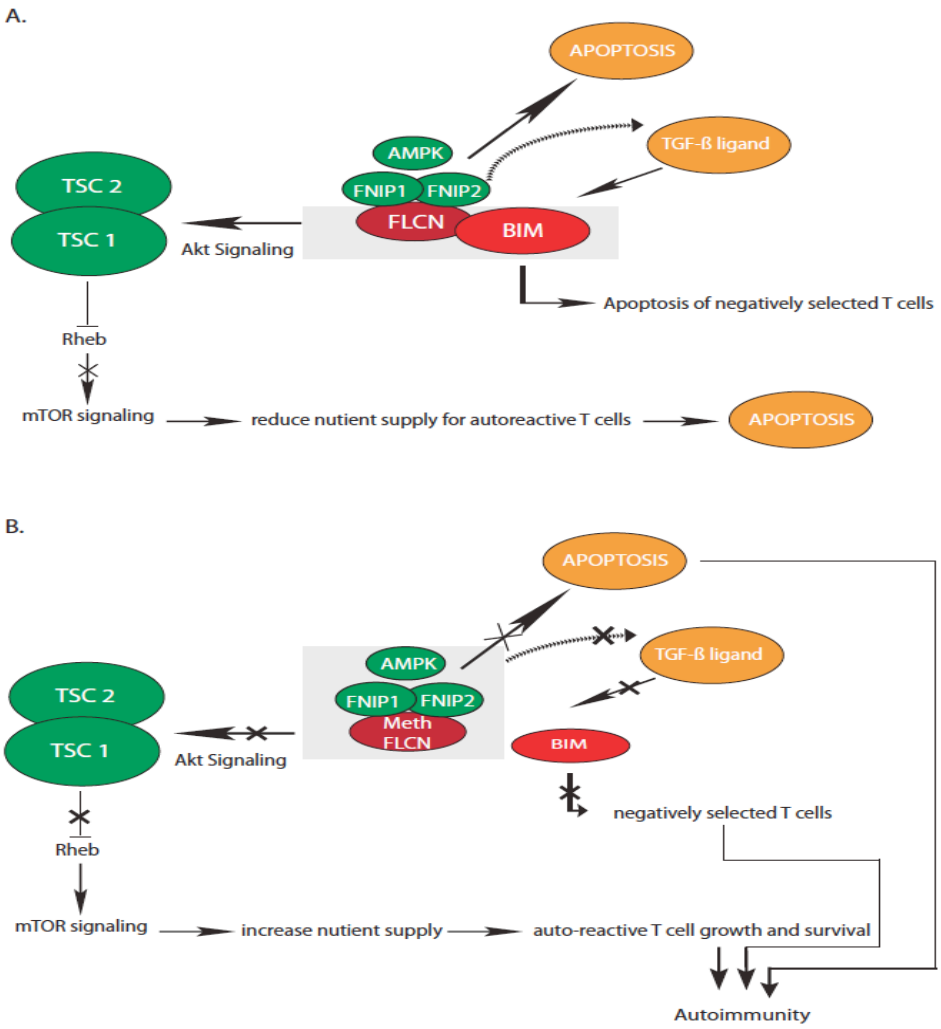

Figure_17: Proposed hypothesis of FLCN gene function in autoimmunity.

A: FLCN gene function in apoptosis through three different signalling processes; AMPK signalling, Akt signalling and TGF-ß signalling pathway might be involved in elimination process of auto reactive T-cells from both systemic and organ specific autoimmune patients. B: Impair FLCN expression no longer be able to eliminate T-cells by apoptosis, which are selected by negative selection and developing autoimmunity.

Taken together, the results presented in this thesis contribute to the development of a MSP based screening approach to analyze genomic regions that are differentially methylated in patients with AAD. As it is possible to analyze relatively many samples at the same time, the goal is that large cohorts of both AAD patients and patients with other autoimmune diseases can be screened. Such studies will contribute to our understanding of the epigenetic signatures of different cohorts, and will also possibly reveal epigenetics similarities or dissimilarities between groups suffering from different autoimmune diseases. However, although more genomic regions should be analyzed before concluding, the results obtained on *FLCN* indicate that it will be necessary to develop qMSP to differentiate between hyper and hypomethylated regions. Future experiments will also focus on the relative functional consequences of an aberrant methylation pattern, *i.e.* it will be determined how overexpression or reprssion of a specific protein will affect T-cells differentiation, proliferation and immune responsiveness among other parameters. Such information is essential with the ultimate in mind; to develop novel therapeutic strategies or biomarkers. Because although most AAD patients in Norway live relatively normal lives after steroid hormone therapy, world wide, autoimmune diseases is a major cause of suffering, illness and death.

References

Arlt, W. and B. Allolio (2003). "Adrenal insufficiency." Lancet **361**(9372): 1881-1893.

Ballestar, E. (2010). "Epigenetics lessons from twins: prospects for autoimmune disease." Clin Rev Allergy Immunol **39**(1): 30-41.

Ballestar, E., M. Esteller, et al. (2006). "The epigenetic face of systemic lupus erythematosus." J Immunol **176**(12): 7143-7147.

Bartolomei, M. S. and A. C. Ferguson-Smith (2011). "Mammalian genomic imprinting." Cold Spring Harb Perspect Biol **3**(7).

Bestor, T. H. (2000). "The DNA methyltransferases of mammals." Hum Mol Genet **9**(16): 2395-2402.

Betterle, C. (2002). "Autoimmune adrenal insufficiency and autoimmune polyendocrine syndromes: Autoantibodies, autoantigens, and their applicability in diagnosis and disease prediction (vol 23, pg 327, 2002)." Endocrine Reviews **23**(4): 579-579.

Betterle, C., F. Lazzarotto, et al. (2004). "Autoimmune polyglandular syndrome Type 2: the tip of an iceberg?" Clinical and Experimental Immunology **137**(2): 225-233.

Bouillet, P., J. F. Purton, et al. (2002). "BH3-only Bcl-2 family member Bim is required for apoptosis of autoreactive thymocytes (vol 415, pg 922, 2002)." Nature **418**(6893): 108-108.

Brand, O., S. Gough, et al. (2005). "HLA , CTLA-4 and PTPN22 : the shared genetic master-key to autoimmunity?" Expert Rev Mol Med **7**(23): 1-15.

Brooks, W. H., C. Le Dantec, et al. (2010). "Epigenetics and autoimmunity." Journal of Autoimmunity **34**(3): J207-J219.

Buckner, J. H. (2010). "Mechanisms of impaired regulation by CD4(+)CD25(+)FOXP3(+) regulatory T cells in human autoimmune diseases." Nat Rev Immunol **10**(12): 849-859.

Burk, C. J., G. Ciocca, et al. (2008). "Addison's disease, diffuse skin, and mucosal hyperpigmenation with subtle "flu-like" symptoms - A report of two cases." Pediatric Dermatology **25**(2): 215-218.

Burk, C. J., G. Ciocca, et al. (2008). "Addison's disease, diffuse skin, and mucosal hyperpigmenation with subtle "flu-like" symptoms--a report of two cases." Pediatr Dermatol **25**(2): 215-218.

Carter, C. J. (2011). "Schizophrenia: a pathogenetic autoimmune disease caused by viruses and pathogens and dependent on genes." J Pathog **2011**: 128318.

Cash, T. P., J. J. Gruber, et al. (2011). "Loss of the Birt-Hogg-Dube tumor suppressor results in apoptotic resistance due to aberrant TGFbeta-mediated transcription." Oncogene **30**(22): 2534-2546.

Coles, A. J., S. Thompson, et al. (2005). "Dehydroepiandrosterone replacement in patients with Addison's disease has a bimodal effect on regulatory (CD4(+)CD25(hi) and CD4(+)FoxP3(+)) T cells." European Journal of Immunology **35**(12): 3694-3703.

Dean, W., F. Santos, et al. (2003). "Epigenetic reprogramming in early mammalian development and following somatic nuclear transfer." Semin Cell Dev Biol **14**(1): 93-100.

Deaton, A. M. and A. Bird (2011). "CpG islands and the regulation of transcription." Genes Dev **25**(10): 1010-1022.

Delcuve, G. P., M. Rastegar, et al. (2009). "Epigenetic control." J Cell Physiol **219**(2): 243-250.

Dorval, K. M., K. G. Wigg, et al. (2007). "Association of the glutamate receptor subunit gene GRIN2B with attention-deficit/hyperactivity disorder." Genes Brain Behav **6**(5): 444-452.

Dowdy, S. C., B. S. Gostout, et al. (2005). "Biallelic methylation and silencing of paternally expressed gene 3 (PEG3) in gynecologic cancer cell lines." Gynecologic Oncology **99**(1): 126-134.

Ehrlich, M., K. Jackson, et al. (2006). "Immunodeficiency, centromeric region instability, facial anomalies syndrome (ICF)." Orphanet Journal of Rare Diseases **1**.

Erichsen, M. M., K. Lovas, et al. (2009). "Normal overall mortality rate in Addison's disease, but young patients are at risk of premature death." European Journal of Endocrinology **160**(2): 233-237.

Feng, W., R. T. Marquez, et al. (2008). "Imprinted tumor suppressor genes ARHI and PEG3 are the most frequently down-regulated in human ovarian cancers by loss of heterozygosity and promoter methylation." Cancer **112**(7): 1489-1502.

Floess, S., J. Freyer, et al. (2007). "Epigenetic control of the foxp3 locus in regulatory T cells." Plos Biology **5**(2): 169-178.

Fraga, M. F., E. Ballestar, et al. (2005). "Loss of acetylation at Lys16 and trimethylation at Lys20 of histone H4 is a common hallmark of human cancer." Nature Genetics **37**(4): 391-400.

Freeman, M. and A. P. Weetman (1992). "T-Cell and B-Cell Reactivity to Adrenal Antigens in Autoimmune Addisons-Disease." Clinical and Experimental Immunology **88**(2): 275-279.

Frommer, M., L. E. McDonald, et al. (1992). "A genomic sequencing protocol that yields a positive display of 5-methylcytosine residues in individual DNA strands." Proc Natl Acad Sci U S A **89**(5): 1827-1831.

Gardiner-Garden, M. and M. Frommer (1987). "CpG islands in vertebrate genomes." J Mol Biol **196**(2): 261-282.

Gartler, S. M. and M. A. Goldman (2001). "Biology of the X chromosome." Current Opinion in Pediatrics **13**(4): 340-345.

Gombos, Z., R. Hermann, et al. (2007). "Analysis of extended human leukocyte antigen haplotype association with Addison's disease in three populations." European Journal of Endocrinology **157**(6): 757-761.

Gregersen, P. K., J. Silver, et al. (1987). "The Shared Epitope Hypothesis - an Approach to Understanding the Molecular-Genetics of Susceptibility to Rheumatoid-Arthritis." Arthritis and Rheumatism **30**(11): 1205-1213.

Grigera, P. R., L. Ma, et al. (2012). "Mass spectrometric analysis identifies a cortactin-RCC2/TD60 interaction in mitotic cells." J Proteomics **75**(7): 2153-2159.

Gronski, M. A., J. M. Boulter, et al. (2004). "TCR affinity and negative regulation limit autoimmunity." Nature Medicine **10**(11): 1234-1239.

Hamza, T. H., C. P. Zabetian, et al. (2010). "Common genetic variation in the HLA region is associated with late-onset sporadic Parkinson's disease." Nat Genet **42**(9): 781-785.

Handel, A. E., G. C. Ebers, et al. (2010). "Epigenetics: molecular mechanisms and implications for disease." Trends Mol Med **16**(1): 7-16.

Hardie, D. G. (2004). "The AMP-activated protein kinase pathway - new players upstream and downstream." Journal of Cell Science **117**(23): 5479-5487.

Hartman, T. R., E. Nicolas, et al. (2009). "The role of the Birt-Hogg-Dube protein in mTOR activation and renal tumorigenesis." Oncogene **28**(13): 1594-1604.

Hasumi, H., M. Baba, et al. (2008). "Identification and characterization of a novel folliculin-interacting protein FNIP2." Gene **415**(1-2): 60-67.

Hong, S. B., H. Oh, et al. (2010). "Inactivation of the FLCN tumor suppressor gene induces TFE3 transcriptional activity by increasing its nuclear localization." PLoS One **5**(12): e15793.

Hong, S. B., H. Oh, et al. (2010). "Tumor suppressor FLCN inhibits tumorigenesis of a FLCN-null renal cancer cell line and regulates expression of key molecules in TGF-beta signaling." Mol Cancer **9**: 160.

Hudon, V., S. Sabourin, et al. (2010). "Renal tumour suppressor function of the Birt-Hogg-Dube syndrome gene product folliculin." J Med Genet **47**(3): 182-189.

Hughes, S. and J. L. Jones (2007). "The use of multiple displacement amplified DNA as a control for methylation specific PCR, pyrosequencing, bisulfite sequencing and methylation-sensitive restriction enzyme PCR." Bmc Molecular Biology **8**.

Illingworth, R. S., U. Gruenewald-Schneider, et al. (2010). "Orphan CpG islands identify numerous conserved promoters in the mammalian genome." PLoS Genet **6**(9).

Invernizzi, P., S. Pasini, et al. (2009). "Female predominance and X chromosome defects in autoimmune diseases." Journal of Autoimmunity **33**(1): 12-16.

Irizarry, R. A., C. Ladd-Acosta, et al. (2009). "The human colon cancer methylome shows similar hypo- and hypermethylation at conserved tissue-specific CpG island shores." Nature Genetics **41**(2): 178-186.

Jacobson, D. L., S. J. Gange, et al. (1997). "Epidemiology and estimated population burden of selected autoimmune diseases in the United States." Clinical Immunology and Immunopathology **84**(3): 223-243.

Javierre, B. M., M. Esteller, et al. (2008). "Epigenetic connections between autoimmune disorders and haematological malignancies." Trends in Immunology **29**(12): 616-623.

Jeffries, M. A., M. Dozmorov, et al. (2011). "Genome-wide DNA methylation patterns in CD4+ T cells from patients with systemic lupus erythematosus." Epigenetics **6**(5): 593-601.

Jia, J., A. Pekowska, et al. (2010). "Assessing the efficiency and significance of Methylated DNA Immunoprecipitation (MeDIP) assays in using in vitro methylated genomic DNA." BMC Res Notes **3**: 240.

Kohda, T., A. Asai, et al. (2001). "Tumour suppressor activity of human imprinted gene PEG3 in a glioma cell line." Genes to Cells **6**(3): 237-247.

Kont, V., A. Murumagi, et al. (2011). "DNA methylation signatures of the AIRE promoter in thymic epithelial cells, thymomas and normal tissues." Molecular Immunology **49**(3): 518-526.

Kouzarides, T. (2007). "Chromatin modifications and their function." Cell **128**(4): 693-705.

Kristensen, L. S., T. Mikeska, et al. (2008). "Sensitive Melting Analysis after Real Time-Methylation Specific PCR (SMART-MSP): high-throughput and probe-free quantitative DNA methylation detection." Nucleic Acids Res **36**(7): e42.

Krohn, K., R. Uibo, et al. (1992). "Identification by Molecular-Cloning of an Autoantigen Associated with Addisons-Disease as Steroid 17-Alpha-Hydroxylase." Lancet **339**(8796): 770-773.

Lal, G. and J. S. Bromberg (2009). "Epigenetic mechanisms of regulation of Foxp3 expression." Blood **114**(18): 3727-3735.

Li, E., T. H. Bestor, et al. (1992). "Targeted Mutation of the DNA Methyltransferase Gene Results in Embryonic Lethality." Cell **69**(6): 915-926.

Li, Y., M. Zhao, et al. (2011). "Abnormal DNA methylation in CD4+ T cells from people with latent autoimmune diabetes in adults." Diabetes Res Clin Pract **94**(2): 242-248.

Li, Y. J., M. Zhao, et al. (2011). "Abnormal DNA methylation in CD4(+) T cells from people with latent autoimmune diabetes in adults." Diabetes Research and Clinical Practice **94**(2): 242-248.

Lim, T. H., R. Fujikane, et al. (2012). "Activation of AMP-activated protein kinase by MAPO1 and FLCN induces apoptosis triggered by alkylated base mismatch in DNA." DNA Repair (Amst) **11**(3): 259-266.

Lovas, K. and E. S. Husebye (2005). "Addison's disease." Lancet **365**(9476): 2058-2061.

Ludwig, H., M. Eibl, et al. (1976). "Cellular and Humoral Immunity to Adrenal Antigens in Patients with Idiopathic Addisons-Disease." Zeitschrift Fur Immunitatsforschung-Immunobiology **152**(3): 179-189.

Maas, K., S. Chan, et al. (2002). "Cutting edge: molecular portrait of human autoimmune disease." J Immunol **169**(1): 5-9.

Maclaren, N. K. and W. J. Riley (1986). "Inherited susceptibility to autoimmune Addison's disease is linked to human leukocyte antigens-DR3 and/or DR4, except when associated with type I autoimmune polyglandular syndrome." J Clin Endocrinol Metab **62**(3): 455-459.

Marrack, P., J. Kappler, et al. (2001). "Autoimmune disease: why and where it occurs." Nature Medicine **7**(8): 899-905.

Martin, D. I. K., R. Ward, et al. (2005). "Germline epimutation: A basis for epigenetic disease in humans." Cooley's Anemia Eighth Symposium **1054**: 68-77.

Maunakea, A. K., R. P. Nagarajan, et al. (2010). "Conserved role of intragenic DNA methylation in regulating alternative promoters." Nature **466**(7303): 253-U131.

Meda, F., M. Folci, et al. (2011). "The epigenetics of autoimmunity." Cell Mol Immunol **8**(3): 226-236.

Myhre, A. G., D. E. Undlien, et al. (2002). "Autoimmune adrenocortical failure in Norway autoantibodies and human leukocyte antigen class II associations related to clinical features." Journal of Clinical Endocrinology & Metabolism **87**(2): 618-623.

Nair, S. S., M. W. Coolen, et al. (2011). "Comparison of methyl-DNA immunoprecipitation (MeDIP) and methyl-CpG binding domain (MBD) protein capture for genome-wide DNA methylation analysis reveal CpG sequence coverage bias." Epigenetics **6**(1): 34-44.

Nerup, J., V. Andersen, et al. (1969). "Anti-adrenal, cellular hypersensitivity in Addison's disease." Clinical and Experimental Immunology **4**(4): 355-363.

Nerup, J., V. Andersen, et al. (1970). "Anti-adrenal cellular hypersensitivity in Addison's disease. IV. In vivo and in vitro investigations on the mitochondrial fraction." Clinical and Experimental Immunology **6**(5): 733-739.

Nerup, J. and G. Bendixen (1969). "Anti-adrenal cellular hypersensitivity in Addison's disease. 3. Species-specificity and subcellular localization of the antigen." Clinical and Experimental Immunology **5**(4): 355-364.

Nerup, J. and G. Bendixen (1969). "Anti-adrenal cellular hypersensitivity in Addison's disease. II. Correlation with clinical and serological findings." Clinical and Experimental Immunology **5**(4): 341-353.

Neufeld, M., N. K. Maclaren, et al. (1981). "Two types of autoimmune Addison's disease associated with different polyglandular autoimmune (PGA) syndromes." Medicine (Baltimore) **60**(5): 355-362.

Nossal, G. J. V. (2001). "A purgative mastery." Nature **412**(6848): 685-686.

Okano, M., D. W. Bell, et al. (1999). "DNA methyltransferases Dnmt3a and Dnmt3b are essential for de novo methylation and mammalian development." Cell **99**(3): 247-257.

Palmke, N., D. Santacruz, et al. (2011). "Comprehensive analysis of DNA-methylation in mammalian tissues using MeDIP-chip." Methods **53**(2): 175-184.

Paulsen, M. and A. C. Ferguson-Smith (2001). "DNA methylation in genomic imprinting, development, and disease." Journal of Pathology **195**(1): 97-110.

Pellegrini, M., G. Belz, et al. (2003). "Shutdown of an acute T cell immune response to viral infection is mediated by the proapoptotic Bcl-2 homology 3-only protein Bim." Proceedings of the National Academy of Sciences of the United States of America **100**(24): 14175-14180.

Polansky, J. K., K. Kretschmer, et al. (2008). "DNA methylation controls Foxp3 gene expression." Eur J Immunol **38**(6): 1654-1663.

Potthoff, M. J. and E. N. Olson (2007). "MEF2: a central regulator of diverse developmental programs." Development **134**(23): 4131-4140.

Quadri, M., A. Federico, et al. (2012). "Mutations in SLC30A10 Cause Parkinsonism and Dystonia with Hypermanganesemia, Polycythemia, and Chronic Liver Disease." American Journal of Human Genetics **90**(3): 467-477.

Rabinowe, S. L., R. A. Jackson, et al. (1984). "Ia-Positive Lymphocytes-T in Recently Diagnosed Idiopathic Addisons-Disease." American Journal of Medicine **77**(4): 597-601.

Ramsahoye, B. H., D. Biniszkiewicz, et al. (2000). "Non-CpG methylation is prevalent in embryonic stem cells and may be mediated by DNA methyltransferase 3a." Proceedings of the National Academy of Sciences of the United States of America **97**(10): 5237-5242.

Rand, K., W. Qu, et al. (2002). "Conversion-specific detection of DNA methylation using real-time polymerase chain reaction (ConLight-MSP) to avoid false positives." Methods **27**(2): 114-120.

Robertson, K. D. (2005). "DNA methylation and human disease." Nat Rev Genet **6**(8): 597-610.

Rodrigues, H. M., A. Jungel, et al. (2009). "Innate immunity, epigenetics and autoimmunity in rheumatoid arthritis." Molecular Immunology **47**(1): 12-18.

Sapolsky, R. M., L. M. Romero, et al. (2000). "How do glucocorticoids influence stress responses? Integrating permissive, suppressive, stimulatory, and preparative actions." Endocrine Reviews **21**(1): 55-89.

Sardiello, M., M. Palmieri, et al. (2009). "A Gene Network Regulating Lysosomal Biogenesis and Function." Science **325**(5939): 473-477.

Shen, L., Y. Kondo, et al. (2007). "Genome-wide profiling of DNA methylation reveals a class of normally methylated CpG island promoters." PLoS Genet **3**(10): 2023-2036.

Soderbergh, A., J. Gustafsson, et al. (2006). "Autoantibodies linked to autoimmune polyendocrine syndrome type I are prevalent in Down syndrome." Acta Paediatrica **95**(12): 1657-1660.

Spies, T. (2002). "Induction of T cell alertness by bacterial colonization of intestinal epithelium." Proceedings of the National Academy of Sciences of the United States of America **99**(5): 2584-2586.

Stephens, H. A. F. (2001). "MICA and MICB genes: can the enigma of their polymorphism be resolved?" Trends in Immunology **22**(7): 378-385.

Suzuki, M., M. Oda, et al. (2011). "Late-replicating heterochromatin is characterized by decreased cytosine methylation in the human genome." Genome Res **21**(11): 1833-1840.

Tao, R., E. F. de Zoeten, et al. (2007). "Deacetylase inhibition promotes the generation and function of regulatory T cells." Nature Medicine **13**(11): 1299-1307.

Ten, S., M. New, et al. (2001). "Addison's disease 2001." Journal of Clinical Endocrinology & Metabolism **86**(7): 2909-2922.

Tuschl, K., P. T. Clayton, et al. (2012). "Syndrome of Hepatic Cirrhosis, Dystonia, Polycythemia, and Hypermanganesemia Caused by Mutations in SLC30A10, a

Manganese Transporter in Man." American Journal of Human Genetics **90**(3): 457-466.

Umetani, N., M. F. G. de Maat, et al. (2005). "Synthesis of universal unmethylated control DNA by nested whole genome amplification with phi 29 DNA polymerase." Biochemical and Biophysical Research Communications **329**(1): 219-223.

Veldhoen, M. and J. H. Duarte (2010). "The aryl hydrocarbon receptor: fine-tuning the immune-response." Curr Opin Immunol **22**(6): 747-752.

Verona, R. I., M. R. Mann, et al. (2003). "Genomic imprinting: intricacies of epigenetic regulation in clusters." Annu Rev Cell Dev Biol **19**: 237-259.

Vocke, C. D., Y. F. Yang, et al. (2005). "High frequency of somatic frameshift BHD gene mutations in Birt-Hogg-Dube-associated renal tumors." Journal of the National Cancer Institute **97**(12): 931-935.

Wang, L., E. F. de Zoeten, et al. (2009). "Immunomodulatory effects of deacetylase inhibitors: therapeutic targeting of FOXP3+ regulatory T cells." Nat Rev Drug Discov **8**(12): 969-981.

Weaver, J. R., M. Susiarjo, et al. (2009). "Imprinting and epigenetic changes in the early embryo." Mamm Genome **20**(9-10): 532-543.

Weber, M., J. J. Davies, et al. (2005). "Chromosome-wide and promoter-specific analyses identify sites of differential DNA methylation in normal and transformed human cells." Nat Genet **37**(8): 853-862.

Weber, M. and D. Schubeler (2007). "Genomic patterns of DNA methylation: targets and function of an epigenetic mark." Curr Opin Cell Biol **19**(3): 273-280.

Weng, Y. I., T. H. Huang, et al. (2009). "Methylated DNA immunoprecipitation and microarray-based analysis: detection of DNA methylation in breast cancer cell lines." Methods Mol Biol **590**: 165-176.

Wilker, P. R., M. Kohyama, et al. (2008). "Transcription factor Mef2c is required for B cell proliferation and survival after antigen receptor stimulation." Nature Immunology **9**(6): 603-612.

Winqvist, O., J. Gustafsson, et al. (1993). "Two different cytochrome P450 enzymes are the adrenal antigens in autoimmune polyendocrine syndrome type I and Addison's disease." J Clin Invest **92**(5): 2377-2385.

Zhang, M. S., J. N. Kimatu, et al. (2010). "DNA cytosine methylation in plant development." Journal of Genetics and Genomics **37**(1): 1-12.

Zhou, Y., X. Qiu, et al. (2011). "Histone modifications and methyl-CpG-binding domain protein levels at the TNFSF7 (CD70) promoter in SLE CD4+ T cells." Lupus **20**(13): 1365-1371.

Zuo, T., B. Tycko, et al. (2009). "Methods in DNA methylation profiling." Epigenomics **1**(2): 331-345.

Appendix I

1.6.3 Methylated DNA immunoprecipitation microarray (MeDIP-chip)

Methylated DNA Immunoprecipitation (MeDIP) is a genome-wide, high-resolution approach to detect differently methylated genomic regions in DNA samples. The method was developed by Weber et al (Weber, Davies et al. 2005), and can be combined with large-scale analysis. The basic principle is the enrichment of methylated DNA with an antibody that specifically binds to 5mC after sonication of purified genomic DNA *(Palmke, Santacruz et al. 2011)*. The enriched methylated DNA then can be combined DNA microarrays (MeDIP-chip) or high throughput sequencing (MeDIP-seq). MeDIP is also suitable for allele-specific studies by combining it with PCR. Though MeDIP is a relatively efficient method to detect methylated DNA, the denaturation step can make the genomic DNA fragile or degraded and low quality DNA will remain for subsequent studies. Antibody specificity can also be problem, but all of these obstacles are greatly reduced in the MeDIP kits that are now available. Moreover, DNA sonication instead of denaturation in the initial step enhances the protocol. Methylated DNA-Binding protein (MBDCap) can be used as an alternative to antibodies against 5mC. Both antibodies will precipitate methylated DNA and are suitable for detecting DMRs (Differentially Methylated Region). MBDCap works better for genomic regions with higher CpG density, which was not a requirement for our experimental design. MBDCap also requires more DNA, and the protocol is more cumbersome (Nair, Coolen et al. 2011). The overall workflow of MeDIP-chip is presented in figure_18.

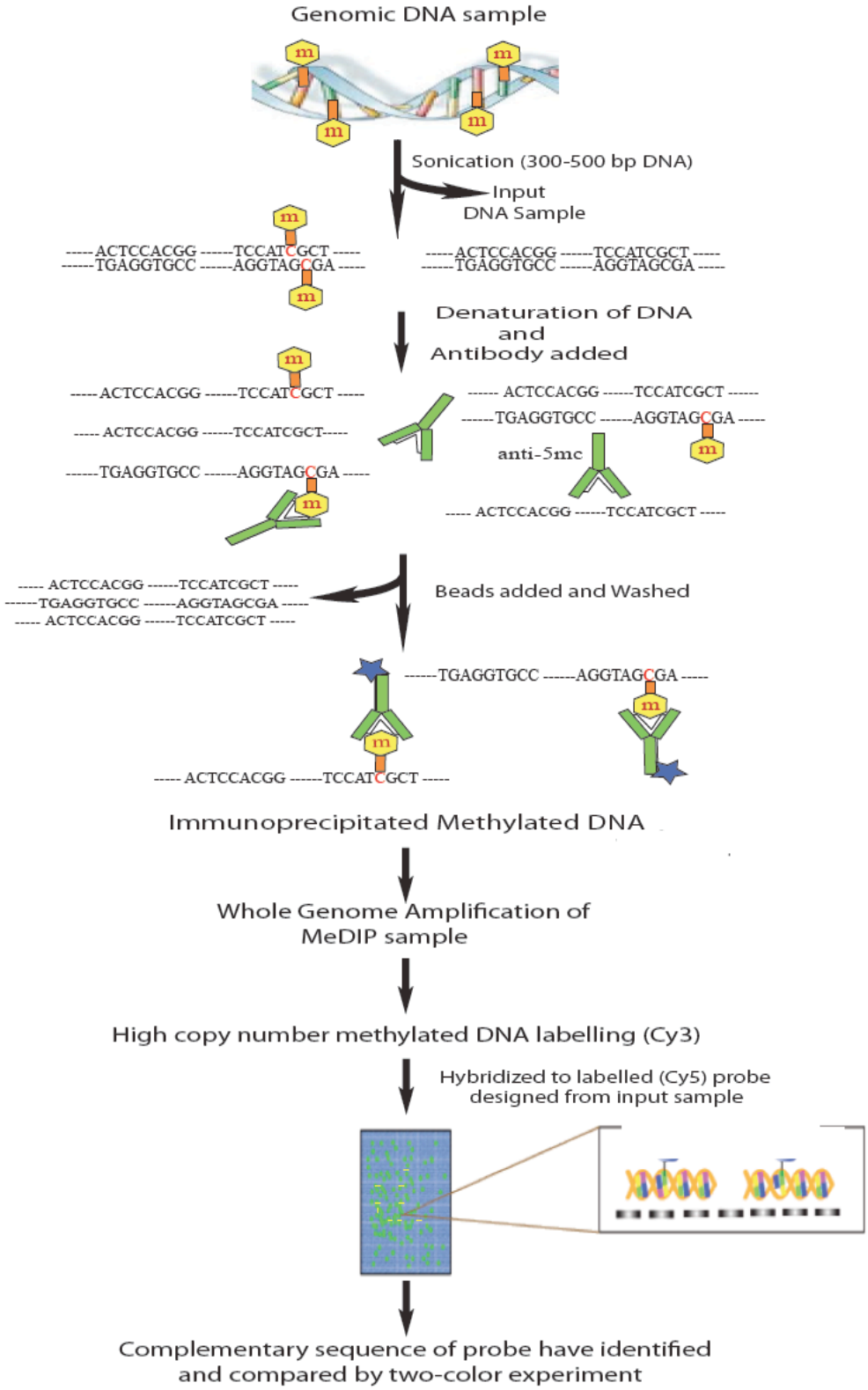

Figure_18: Workflow of the methylated DNA immunoprecipitation microarray (MeDIP-chip). Desired fragments length was generated by sonication and incubated with an antibody directed against 5mC and methylated DNA is isolated by immunoprecipitation. Whole genome amplification was introduced to get sufficient amount of DNA for quantification the methylated fractions by comparing with two-colour experiment in microarray analysis.

MeDIP-chip is a microarray-based genomic survey used in DNA methylation analysis because of its high throughput manner. The method has successfully been applied both in animals and plants to identify differences in DNA methylation (Weng, Huang et al. 2009). Relatively large amounts of DNA are required for array hybridization, but the outcome from the MeDIP is usually in 50-100 ng in range. To obtain enough DNA, whole genome amplification (WGA) was performed before microarray to increase the copy number of enriched genomic sequences (Weber, Davies et al. 2005). It is critical that all loci are amplified equally to ensure unbiased hybridization to the array. WGA also simplifies the analysis of DNA from tissues that are limited, but "false positive" results for some specific regions might be experienced as a limitation for MeDIP-chip (Jia, Pekowska et al. 2010). A potential limitation of MeDIP is also the fact that large genomic regions with a high CpG content will be more efficient precipitated than a region with few CpG sites. Depending on the purpose of the study this might be a limitation, and moreover as a result of this bias, validated sequences could be just opposite in methylation status to the same genomic region of methylated DNA. Genomic DNA is sheared to low molecular weight fragment after sonication, with an average size of 400 bp. Therefore, this is not disadvantage of the method but need to simplify. Other than this particular condition, MeDIP-chip is adequate for DNA methylation analysis. Thereafter, multiple accessibility for data validation inspired to chose the method as well.

Appendix II

The region obtained from the result of Human DNA Methylation 2.1M Delux Promoter array analysis is corresponding to the gene and gene description listed here according to UCSC genome browser (http://genome.ucsc.edu/); in the first column, chromosomal location of each gene have mentioned. The mean in the second column describes the score of relative methylation in this region. The value over two is defined as significantly methylated. This score is the case group and all controls has scored below two in this region meaning that the controls are not methylated.

Table_XXII: List of genes from MeDIP-chip result

CHR	MEAN	GEN	DESCRIPTION
chr1	3.306	PRDM2	PR domain containing 2, with ZNF domain
chr1	3.543	RCC2	Regulator of chromosome condensation 2
chr1	2.932	ZNF643	zinc finger protein 643
chr1	2.640	SLC30A10	Solute carrier family 30, member 10
chr10	2.893	GRID1	glutamate receptor, ionotropic, delta 1
chr11	3.192	CARS	cysteinyl-tRNA synthetase
chr16	4.095	LRRC29	leucine rich repeat containing 29
chr17	3.857	FLCN	folliculin
chr2	4.031	HDAC4	histone deacetylase 4
chr21	2.881	FAM83C	NA
chr22	2.983	NF2	neurofibromin 2 (bilateral acoustic neuroma)
chr22	3.196	C22orf23	Chromosome 22 open reading frame 23
chr22	3.102	RP11-19IL9.1	NA
chr5	2.873	BTNL9	butyrophilin-like 9
chr10	2.645	ZA20D1	NA
chr12	2.908	GRIN2B	glutamate receptor, ionotropic, N-methyl D-aspartate 2B
chr14	2.915	STRN3	striatin, calmodulin binding protein 3
chr14	2.905	SETD3	SET domain containing 3
chr16	3.058	ATRNL1	NA
chr16	2.908	LOC197322	hypothetical protein LOC197322
chr17	2.965	ACLY	ATP citrate lyase
chr17	2.933	PSCD1	pleckstrin homology, Sec7 and coiled-coil domains 1(cytohesin 1)
chr18	2.853	NETO1	neuropilin (NRP) and tolloid (TLL)-like 1
chr2	3.242	UGCGL1	UDP-glucose ceramide glucosyltransferase-like 1
chr2	3.010	GDF8	
chr21	2.595	UBE2G2	ubiquitin-conjugating enzyme E2G 2
chr3	3.135	PLD1	phospholipase D1, phosphatidylcholine-specific
chr4	2.980	C4orf8	chromosome 4 open reading frame 8
chr5	3.367	FGF1	fibroblast growth factor 1 (acidic)
chr5	3.487	FGF1	fibroblast growth factor 1 (acidic)
chr6	2.282	WDR27	WD repeat domain 27
chr8	2.832	EXT1	exostoses (multiple) 1